

# Neutrino Oscillations<sup>1</sup>

M.L.Tan '90

Thesis Advisor: Professor K.Jagannathan

May 10, 1990

<sup>1</sup>Submitted to the Department of Physics of Amherst College in partial fulfillment of the requirements for the degree of Bachelor's of Arts with Honors

# Contents

<b>1</b>	<b>MASSIVE NEUTRINOS</b>	<b>5</b>
1.1	Introduction . . . . .	5
	Discovery . . . . .	5
	Flavors and Masses . . . . .	6
1.2	Mass Measurements . . . . .	7
	Previous Experiments . . . . .	7
	Experimental Method . . . . .	8
	Errors . . . . .	10
	Future Experiments . . . . .	10
1.3	Neutrinos from SN1987a . . . . .	11
	Stellar Evolution . . . . .	11
	Neutrino Decay . . . . .	11
	Neutrino Mass Limit . . . . .	12
1.4	Neutrino Oscillations . . . . .	14
	Propagation Eigenstates . . . . .	14
	Vacuum Oscillations . . . . .	15
	Detecting Neutrino Oscillations . . . . .	18
1.5	The Solar Neutrino Problem . . . . .	19
	Possible Solutions . . . . .	21
<b>2</b>	<b>MATTER OSCILLATIONS</b>	<b>23</b>
2.1	Matter Oscillations . . . . .	23
	Propagation in Vacuum . . . . .	23
	Propagation in Matter . . . . .	25
	Varying Density . . . . .	27
	MSW Effect . . . . .	29

3	$\bar{\nu}_e d \rightarrow n n e^+$ CROSS-SECTION	30
3.1	Deuterium Reactions . . . . .	30
	Neutrino Flux Measurements . . . . .	30
3.2	$\bar{\nu}_e d \rightarrow n n e^+$ Cross Section . . . . .	32
	Previous Work . . . . .	32
	First Approximation . . . . .	35
	Deuterium Ground State . . . . .	36
	Inverse Beta Decay . . . . .	41
	Averaged Cross-Section . . . . .	49
	Kinematic Limits . . . . .	51
	Better Approximation . . . . .	61
3.3	Conclusion . . . . .	62
	Critique . . . . .	62
	Commendation . . . . .	63
A	Computer Programs	66

Like every intellectual pursuit, physics has both a written and an oral tradition. Intuitive modes of thought, inference by analogy, and other strategems that are used in the effort to confront the unknown are transmitted from one generation of practitioners to the next by word of mouth. After the work of creation is over, the results are recorded for posterity in a logically impeccable form, but in a language that is often opaque. The beginner is expected to absorb this written tradition, and only the survivors of this trial-by-ordeal are admitted to circles where the oral tradition is current. We could only hope to strive toward our goal by leaning heavily on the oral tradition... we believe that this tradition plays an essential role not only in the creation of physics, but also in the search for a deeper understanding...

Gottfried and Weisskopf  
*Concepts of Particle Physics, Vol. 1*

## Preface

More than just to learn to do a field theory calculation, the aim of the thesis has been to expose myself to contemporary issues in particle and nuclear physics. To this end I have studied a series of articles on solar neutrinos, neutrino mass and oscillation, neutrino detection experiments, etc, and presented the knowledge in the first and second chapters—much in a fashion that reflects my intuitive understanding of the material. Perhaps herein lies the strength of the presentation, for the use of rough and ready analogies, the press for the idea and the motivation rather than the particulars will surely appeal to non-specialists in the field. Still a journal it is not and a standard of scientific rigor will be apparent in the writing (and indeed will be presumed in the reader).

The stage is then set for the third chapter which records the effort to calculate the cross-section for the neutrino-deuterium reaction

$$\bar{\nu}_e + d \rightarrow n + n + e^+$$

relevant to many neutrino detection experiments. In a rather picturesque model of the interaction, the deuteron is regarded as in some sense a system of two ‘orbiting’ particles, viz. a neutron and a proton, and the antineutrino hits the latter and changes it to a neutron. The calculation is carried through without accounting for the Pauli exclusion of the two final-state neutrons, although an outline of a proper treatment is also provided. The qualified agreement between our results and those published as well as the merits and shortcomings of the method used are also discussed.

I deeply appreciate the guidance of Prof. K.Jagannathan, who had very much sought to raise me into the oral tradition of theoretical physics.

M.L.Tan '90

April 1990



# Chapter 1

## MASSIVE NEUTRINOS

Is the neutrino massless? No established principle affirms this and no credited experiment denied it. Direct measurements have shown that the neutrino is far lighter than all the particles we have discovered. It is entirely possible from these measurements that the neutrino is massless. Indeed there are theories that require massless neutrinos—but many do not. The theoretical aesthetic in general is to regard a massless neutrino as quite accidental; and a deeper reason is to be found if its mass were indeed zero. Thus the neutrino mass issue is an important and unsettled one. In this chapter we will begin to address it by studying some phenomenological aspects of massive neutrino physics and recent experiments to detect neutrino mass.

### 1.1 Introduction

#### Discovery

The neutrino was postulated by Pauli in 1930 to account for the apparent nonconservation of energy in nuclear beta decay. Such decay occurs when a neutron, in a heavy nucleus such as radium, breaks into a proton, an electron and an anti-electron neutrino:

$$n \rightarrow p + e^- + \bar{\nu}_e.$$

If the neutrino were absent, the energy spectrum of the emitted electron (i.e. number versus energy) should be discrete. For the electron energy

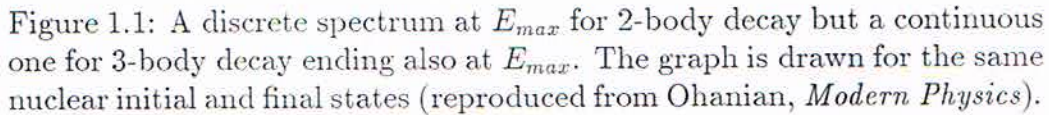


Figure 1.1: A discrete spectrum at  $E_{max}$  for 2-body decay but a continuous one for 3-body decay ending also at  $E_{max}$ . The graph is drawn for the same nuclear initial and final states (reproduced from Ohanian, *Modern Physics*).

is simply the difference between the energies of the parent and daughter nuclei, and energy levels in nuclei were known to be discrete from nuclear scattering experiments (1920s). But the observed spectrum (1927) drops continuously from a maximum equal to the value expected without the neutrino to zero (Figure 1.1). This effect could be explained if a third particle is emitted which shares the energy given to the electron. This particle, the  $\bar{\nu}_e$ , was first detected directly in a reactor experiment (1953). Its mass can be inferred from the energy spectrum; and until recently an upper limit was placed at 46eV[1], or about  $10^{-4}$  times the electron mass.

## Flavors and Masses

There are at least three ‘flavors’ (species) of neutrinos, corresponding to the three types of leptons with which they interact. They are labelled  $\nu_e$ ,  $\nu_\mu$ ,  $\nu_\tau$ , and their anti-particles  $\bar{\nu}_e$ ,  $\bar{\nu}_\mu$ ,  $\bar{\nu}_\tau$ . The  $\nu_e$  is emitted in nuclear beta-decay; the  $\nu_\mu$  in the decay of muons and pions. The  $\nu_\tau$  has never been detected directly but is believed to be emitted in the decay of the tauon. The present limits on the  $\nu_\mu$  and  $\nu_\tau$  masses are  $m_{\nu_\mu} < 250\text{keV}$  and

$m_{\nu_\tau} < 35\text{MeV}$ [2].

Within the standard electroweak theory all neutrinos are assumed to be massless particles with no magnetic moments. It appears that the only parameter to be determined is the total number of neutrino species, which may in fact be three as a recent measurement[22] indicates. But some extensions of this theory to accomplish grand unification with the strong and gravitational interactions require non-zero neutrino masses. Theoretically the prejudice is against a zero mass since there is no compelling justification for it<sup>1</sup>. Indeed recent experiments (section 1.2) suggest that the  $\nu_e$  is possibly massive.

The massive neutrino is associated with a quantum mechanical process known as neutrino oscillation (section 1.4), which is the transformation of neutrinos of one flavor into another, and which will not occur if they are massless. This transformation may explain a 20-year old discrepancy between the number of neutrinos from the Sun detected on Earth and the number expected from theoretical solar models. Non-zero neutrino masses also have implications for cosmology and theories of the evolution of the universe. With the recent advent of high-resolution spectrometers having a mass sensitivity of 10eV or better, the massive neutrino has become an issue of much theoretical and experimental interest.

## 1.2 Mass Measurements

### Previous Experiments

The high-energy end of the spectrum for nuclear  $\beta$ -decay is sensitive to neutrino mass. The paradigm has been to determine  $m_{\nu_e}$  from the spectrum of  $\beta$ -decay in tritium

$${}^3\text{H} \rightarrow {}^3\text{He} + e^- + \nu_e.$$

The trend had been for decreasing upper limits to  $m_{\nu_e}$  as measurements became more accurate. The expectation was that  $m_{\nu_e}$  may indeed be zero. Then a recent experiment by V.A.Lubimov et al[4] (Moscow 1980) gave a positive *lower* limit

$$17\text{eV} < m_{\nu_e} < 40\text{eV} \quad (90\% \text{ confidence level})$$

---

<sup>1</sup>The photon is the only particle acknowledged to be massless, with good reason.



and a best fit value<sup>2</sup> of  $\sim 30\text{eV}$ . However, conflicting claims were subsequently made by M.Fritschi et al[5] (Zurich 1986), H.Kawakami et al[6] (Tokyo 1987), and D.L.Wark et al[7] (Los Alamos 1987):

$m < 18\text{eV}$ (90%)	Zurich
$m < 17\text{eV}$ (90%)	Tokyo
$m < 27\text{eV}$ (95%)	Los Alamos.

## Experimental Method

In these experiments, electrons emitted from a tritium source (solid or gaseous) are guided into a spectrometer which analyzes the distribution of energies by magnetic focussing techniques. To observe a mass effect, the spectrum must be measured accurately up to a few neutrino masses before the end-point  $E_0$  which occurs at about  $18.6\text{keV}$ . It is difficult to measure the end-point directly, since the count rate there is comparable to the background. What is done is to fit the measured spectrum (including the fuzzy data at the end-point—see Figure 1.2) to a known function, and then statistically infer a value for  $E_0$ . The function is essentially

$$N(E) = G + A \int_0^{E_0} S(E', m_\nu, E_0) R(E', E) [1 + \alpha_1(E_0 - E') + \alpha_2(E_0 - E')^2 + \dots] dE'.$$

$N(E)$  is the number of electrons detected with energy  $E$ .  $S(E', m_\nu, E_0)$  is the expected spectrum (i.e. number *emitted* with energy  $E'$ ) calculated based on the density of final states for  ${}^3\text{He}$ . Energy loss as the electron traverses the source and backscattering processes, in which the electron is deflected by more than  $90^\circ$  from its original direction and is not detected because the spectrometer only collects electrons from a limited solid angle, will affect the spectrum; they are also incorporated into  $S(E', m_\nu, E_0)$ .  $A$  normalizes the sum to the total number of electrons.  $G$  is the noise level due to cosmic rays and radioactive contamination of the spectrometer. The series parametrized by  $\alpha_{1,2}$  is an ‘efficiency correction’ that accounts for the electron detecting mechanism being made to be most efficient at the end-point  $E_0$ . It corrects ‘undercounting’ at energies away from  $E_0$ , where the

---

<sup>2</sup>90% confidence level means  $P(17\text{eV} < m < 40\text{eV}) = 0.90$

Figure 1.2: The data close to the end-point of the  $^3\text{H}$  spectrum reproduced from the Tokyo experiment.

efficiency (i.e. ratio of number detected and emitted at each energy) is lower.

$R(E', E)$  is the spectrometer response function, i.e. the probability of detecting an electron with energy  $E$  when it really has energy  $E'$ . It is determined by putting in place of the tritium a field-emission electron gun or some other type of source whose emission is controllable or well-known.  $R(E, E')$ , which is regarded as the fraction of detected  $E$  electrons that are really  $E'$  electrons, drops quickly to zero as  $|E - E'|$  becomes large. It is usually approximated by a gaussian centered at  $E$  and  $\sim 10\text{eV}$  wide. This means that each point  $E$  in the output (measured) spectrum has contributions from a *range* of points  $E'$  in the input spectrum. The spectrometer ‘blurs’ the output by spreading out each input point (this also happens in a telescope for instance). Mathematically this blurring is expressed as the convolution of  $S(E', m_\nu, E_0)$  with  $R(E', E)$ , i.e. the integration over  $E'$ .

The parameters  $G$ ,  $E_0$ ,  $m_\nu$ ,  $A$ ,  $\alpha_{1,2}$  are varied until a best fit to the data is obtained.  $\chi^2$  minimization or more sophisticated methods were used, and



Monte-Carlo simulations of the experiment were also performed to verify the fairness of the fit.

## Errors

Uncertainties in the measurement are mainly (a) statistical, i.e. those arising from the fitting procedure; and (b) resolutional, i.e. those arising from the finite width of the spectrometer response function. Also  $S(E', m_\nu, E_0)$  may be a source of systematic error if the final states of  $^3\text{He}$  are not calculated accurately. In fact both the Moscow and Tokyo experiments used tritium in a complex compound form—respectively valine  $((\text{CH}_3)_2\text{CH}.\text{CH}(\text{NH}_2).\text{COOH})$  and arachidic acid  $(\text{C}_{20}\text{H}_{40}\text{O}_2)$ —and the Zurich experiment used tritium implanted in carbon. The final-state effects are complex and the energy lost by the electron to molecular excitations are comparable to the size of the neutrino mass. Backscattering effects and energy losses as the electron traverses the source are also complicated. The Los Alamos experiment had sought to eliminate the above problems by using free molecular tritium (gaseous source), since its final states are accurately known and the energy losses are small.

## Future Experiments

In view of the above problems, the conflicting mass limits may well be due to systematic errors. A definitive measurement awaits the next generation of experiments[8,9,10]. While still involving the  $\beta$ -spectrum of tritium, they will offer the following improvements:

1. Higher instrument resolution ( $< 15\text{eV}$ ) with electrostatic spectrometers
2. Better statistics by increasing the count rate in the mass sensitive region and reducing backscattering and energy-loss effects using improved tritium sources (thinner, more active)
3. Lower noise-to-signal ratio by carefully differentiating  $\beta$ -decay electrons from background electrons.

## 1.3 Neutrinos from SN1987a

Bursts of neutrinos ( $\nu_e$ ) from Supernova 1987a in the Large Magellanic Cloud were observed on Feb 23 1987 by the Kamiokande-II[12] and IMB[11] water-Cerenkov detectors. The Kamiokande-II recorded 12 neutrino events in an interval of 12.4 sec, with an average neutrino energy of  $9 \pm 1$  Mev. The IMB recorded 8 events in 5.6 sec, with an average energy of  $14 \pm 2$  Mev[14]. (The two detectors sample different energy ranges). Some implications of these historic observations are:

### Stellar Evolution

The observations are supportive of the current theories of stellar evolution and neutron star formation. The standard stellar model predicts that as fusion reactions in the stellar core led to the formation and nuclear burning of successively heavier elements, a massive star becomes unstable and collapses under its own gravity. The collapse and the ensuing violent outburst, when the outer layers are being ejected while the core is left as a neutron star, is accompanied by two energetic neutrino bursts. The first occurs during the collapse and lasts no more than half a second; the second occurs during the outburst and lasts several seconds. The contiguity in time of the neutrino observations and the first optical sighting<sup>3</sup> gives compelling evidence that neutrinos are indeed released during the supernova stage. Also the average energy of the  $\nu_e$ 's radiated is expected from the standard model to be 10–20MeV[14], which agrees with the observed values.

### Neutrino Decay

A life-time for  $\nu_e$  greater than  $10^4$  years can be inferred, ruling out neutrino decay as an explanation of the observed solar neutrino deficiency (see section 1.6). The total number of neutrinos produced by SN1987a is estimated to be  $\sim 10^{58}$ [14], of which  $\sim 10^{29}$  is directed at the Earth 150,000 light-years away. Even assuming that the two detectors are 100% efficient, no less than  $\sim 10^{16}$  neutrinos must have passed through the Earth. A mean-life  $\tau$  can

---

<sup>3</sup>The neutrinos were in fact observed about 18 hours before the first optical sighting. This is not surprising since light emission increases gradually over many hours, while neutrinos are all emitted within a few seconds.



be inferred from

$$10^{16} \simeq 10^{29} \exp[-(150000 \text{yr}/\gamma)/\tau]$$

giving  $\tau > 10^4/\gamma$  yrs, where  $\gamma = 1/\sqrt{1 - v^2/c^2}$  = ratio of neutrino energy to neutrino mass. Note that  $\gamma$  is there because of time dilation and  $\tau$  is measured in the neutrino's frame. In the earth's frame the mean-life is simply  $10^4$  yrs.

## Neutrino Mass Limit

An upper limit  $m_{\nu_e} < 6\text{eV}$  can be derived from the arrival times and energies of the neutrinos. The calculation due to A.Burrows[14] is essentially the following: If neutrinos are massive, then different energies would correspond to different speeds. A delta function pulse of neutrinos with different energies will disperse temporally as they travel away from the source. From the relationship

$$u^2 = 1 - \frac{m^2}{E^2} \quad (1.1)$$

where the symbols have their usual meanings ( $u$  is velocity,  $c = 1$ ,  $m = m_{\nu_e}$ , etc), we obtain

$$\Delta u = \frac{m^2}{uE^3} \Delta E.$$

And using  $t = D/u$ , where  $D$  is the distance between SN1987a and the earth, we get

$$\begin{aligned} \Delta t &= D \frac{\Delta u}{u^2} \\ &= \left( \frac{D}{u^3} \right) \left( \frac{m^2}{E^2} \right) \left( \frac{\Delta E}{E} \right) \end{aligned} \quad (1.2)$$

where  $\Delta t$  is the lapse in arrival times between two neutrinos of energy  $E$  and  $(E - \Delta E)$ . It can also be regarded as the deviation as a function of  $\Delta E$  from the average arrival time corresponding to the average energy  $E$ . The calculation is more complicated if the neutrinos do not leave at the same time. A distribution of departure times would map into a distribution of arrival times. Equation 1.2 still holds qualitatively, though we might think of different departure times as effectively different  $D$ 's.

Kamiokande-II recorded 5 neutrinos in the first  $\sim 0.5$  seconds. One can ask: Given a value for  $m$ , an energy distribution that (purportedly) characterizes the source, and a time interval  $\tau_s$  in which 5 neutrinos were randomly emitted from the source, what is the probability that these 5 neutrinos will arrive at the detector within a time interval  $\tau_d \leq 0.5$  seconds? Equation (1.2) shows that for a given  $\tau_s$ —i.e. for emissions times that are restricted to within a given  $\tau_s$ —the bigger  $m$  is the more likely it is to cause a wider spread in arrival times. That is, for large  $m$ , and barring unduely small  $\Delta E$ , each neutrino will have a  $\Delta t$  that is large; and so even if  $\tau_s$  were small,  $\tau_d$  is still likely to be large. Also it is unlikely that neutrinos emitted over a long interval ( $\tau_s \gg \tau_d$ ) will converge into 0.5 seconds on arrival. Thus the probability  $P(\tau_d \leq 0.5\text{s})$  as a function of  $m$  and  $\tau_s$  decreases for increasing  $m$  and  $\tau_s$ . This is indicated in Figure 1.3 reproduced from Burrows[14], who obtained it using a series of Monte-Carlo calculations. From the figure it is clear that a mass  $m > 7\text{eV}$  and an emission interval  $\tau_s > 1$  sec effectively rule out the observation of 5 events in 0.5 sec.

The Kamiokande-II detector gave not only the arrival times but also the energies of the neutrinos. A specific arrival time and energy together with a given mass imply a specific emission time (cf. equation (1.1), which gives the velocity and hence the time of travel). Thus the emission interval  $\tau_s$  corresponding to the first 5 events can be derived as a function of  $m$ . So  $P(\tau_d \leq 0.5)$  instead of being a function of both  $m$  and  $\tau_s$  is in fact a function of  $m$  only. Below is a table of  $P(\tau_d \leq 0.5)$  and  $m$  values reproduced from Burrows, which shows that for  $m > 6\text{eV}$ ,  $P(\tau_d \leq 0.5) < 0.01$ . That is, it is nearly impossible for 5 neutrinos of mass  $m > 6\text{eV}$  to arrive within 0.5 sec. Hence an upper limit of 6eV (99% confidence level) can be placed on  $m$ . Note however that the above analysis does not prescribe a non-zero  $m$ . In fact for maximum probability, it may as well vanish. The value of 6eV is just what it is—an upper limit.

Figure 1.3: Probability that 5 neutrinos will arrive within 0.5 seconds vs  $\tau_s$  and  $m$ .

$P(\tau_d \leq 0.5)$	$m(\text{eV})$
$\sim 1.0$	1
0.99	2
0.76	3
0.19	4
0.05	5
0.01	6
0.002	7
$<.001$	8

## 1.4 Neutrino Oscillations

### Propagation Eigenstates

The  $\nu_e$ ,  $\nu_\mu$ ,  $\nu_\tau$  couple to respectively the  $e$ ,  $\mu$ ,  $\tau$  particles via the weak interaction and are hence classified as leptons, or weak-interaction eigenstates. A neutrino is in general a superposition of  $\nu_e$ ,  $\nu_\mu$ , and  $\nu_\tau$ . It is identified by the way it interacts in a weak process, just as a superposition of the eigenstates of an observable collapses into a single one during measurement. For



example, a capture process  $\nu + d \rightarrow e^- + 2n$  in which an electron is created fixes  $\nu$  as  $\nu_e$ ; and one in which a muon is created fixes  $\nu$  as  $\nu_\mu$  and so forth. Thus  $\nu_e, \nu_\mu, \nu_\tau$  are the right basis for describing weak-interaction processes. But the neutrino is generally not expected to propagate in its weak-interaction eigenstates. The proper basis for describing propagation is a set of mass eigenstates  $\nu_1, \nu_2, \nu_3$ .

## Vacuum Oscillations

The mass eigenstates are related to the weak-interaction eigenstates by a unitary (change-of-basis) transformation. If we consider only two-neutrino mixing, the transformation is

$$\begin{pmatrix} \nu_e \\ \nu_\mu \\ \nu_\tau \end{pmatrix} = \begin{pmatrix} \cos \theta & \sin \theta & 0 \\ -\sin \theta & \cos \theta & 0 \\ 0 & 0 & 1 \end{pmatrix} \begin{pmatrix} \nu_1 \\ \nu_2 \\ \nu_3 \end{pmatrix}. \quad (1.3)$$

We have assumed for simplicity that the  $\nu_\tau$  is a pure  $\nu_3$  state, while  $\nu_e$  and  $\nu_\mu$  are each mixtures (linear combinations) of  $\nu_1$  and  $\nu_2$ . Although the most general  $2 \times 2$  unitary matrix has four independent parameters, three of which appear as phase factors, the matrix parametrized by the real mixing angle  $\theta$  will suffice to exhibit the important physical features of neutrino oscillation. The degree of mixing is characterized by  $\theta$ , which is at present an unknown parameter;  $\theta = 0$  implies no mixing (the eigenstates coincide) and  $\theta = \pi/4$  implies maximum mixing (equal portions of  $\nu_1$  and  $\nu_2$ ). Writing (1.3) as separate equations gives

$$|\nu_e\rangle = \cos \theta |\nu_1\rangle + \sin \theta |\nu_2\rangle \quad (1.4)$$

$$|\nu_\mu\rangle = -\sin \theta |\nu_1\rangle + \cos \theta |\nu_2\rangle \quad (1.5)$$

and multiplying (1.3) by the inverse of the mixing matrix gives

$$|\nu_1\rangle = \cos \theta |\nu_e\rangle - \sin \theta |\nu_\mu\rangle \quad (1.6)$$

$$|\nu_2\rangle = \sin \theta |\nu_e\rangle + \cos \theta |\nu_\mu\rangle. \quad (1.7)$$

The mass eigenstates are also eigenstates of energy and momentum. Their time development is given by

$$|\nu_{1,2}(t)\rangle = \exp(-i\hat{H}t)|\nu_{1,2}\rangle = |\nu_{1,2}\rangle \exp(-iE_{1,2}t). \quad (1.8)$$



Now suppose the eigenstate  $|\nu_e\rangle$  is created initially

$$|\nu(t=0)\rangle = |\nu_e\rangle$$

where  $\nu(t)$  denotes a general neutrino state. To describe its propagation, we write it as a superposition of mass eigenstates (equation (1.4)) having equal momenta whose time development is given by (1.8)

$$|\nu(t)\rangle = \cos\theta|\nu_1\rangle \exp(-iE_1t) + \sin\theta|\nu_2\rangle \exp(-iE_2t) \quad (1.9)$$

After travelling for a time  $t$ , the neutrino is detected via a weak-interaction process such as  $\nu + d \rightarrow L + 2n$ , where  $L = e, \mu$ , or  $\tau$  serves to identify  $\nu$ . To see how the neutrino will interact, we use (1.6) and (1.7) to rewrite (1.9) as a superposition of weak-interaction eigenstates

$$\begin{aligned} |\nu(t)\rangle &= [\exp(-iE_1t) \cos^2\theta + \exp(-iE_2t) \sin^2\theta]|\nu_e\rangle \\ &+ [-\exp(-iE_1t) \cos\theta \sin\theta + \exp(-iE_2t) \sin\theta \cos\theta]|\nu_\mu\rangle \end{aligned}$$

which gives the probabilities

$$\begin{aligned} |\langle\nu_e|\nu(t)\rangle|^2 &= 1 - \frac{1}{2} \sin^2 2\theta [1 - \cos(E_2 - E_1)t] \\ &= 1 - \sin^2 2\theta \sin^2 \left[ \frac{(E_2 - E_1)}{2} t \right] \end{aligned} \quad (1.10)$$

$$|\langle\nu_\mu|\nu(t)\rangle|^2 = \sin^2 2\theta \sin^2 \left[ \frac{(E_2 - E_1)}{2} t \right] \quad (1.11)$$

Clearly if  $\theta \neq 0$ , the neutrino that set out as pure  $\nu_e$  will later become a mixture of  $\nu_e$  and  $\nu_\mu$ . It will have some probability of interacting like  $\nu_\mu$  and a reduced probability of interacting like  $\nu_e$ . Because the probabilities are oscillatory functions of time, the  $\nu_e$  is said to have ‘oscillated’ into  $\nu_\mu$ . This is the process of neutrino oscillation—in *vacuum* since we have not examined the dependence of  $\theta$  on the medium.

For relativistic  $\nu_1, \nu_2$ , the probabilities can be simplified by using the approximation  $E = \sqrt{p^2 + m^2} \simeq p + m^2/2p$  (since  $E_i, p_i \gg m_i$ ) and the assumption that  $p_1 = p_2$  to write

$$\begin{aligned} (E_1 - E_2)t &\simeq \left( \frac{m_1^2 - m_2^2}{2p} \right) t \\ &= \frac{\Delta m^2}{2E} l + o(m^4). \end{aligned}$$

Hence, the probabilities, written in terms of an oscillation length  $l_v = 4\pi E/\Delta m^2$ , are

$$|\langle \nu_e | \nu(t) \rangle|^2 = 1 - \sin^2 2\theta \sin^2 \left( \pi \frac{l}{l_v} \right) \quad (1.12)$$

$$|\langle \nu_\mu | \nu(t) \rangle|^2 = \sin^2 2\theta \sin^2 \left( \pi \frac{l}{l_v} \right). \quad (1.13)$$

Note that the period of  $\sin^2$  is  $\pi$ . Energy conservation is not violated as  $\nu_e$  transforms into  $\nu_\mu$  (where  $m_{\nu_e} \neq m_{\nu_\mu}$ ) because they are not eigenstates of energy. The calculation could also have begun with a pure  $\nu_\mu$  and similar results would follow.

The physical picture is this: Suppose a beam of neutrinos begins at a source as pure  $\nu_e$ 's. Along the way some  $\nu_e$ 's transform into  $\nu_\mu$  and vice versa. The probability  $P(\nu \rightarrow \nu_e)$  is the fraction of the beam that remains as  $\nu_e$ , and  $P(\nu \rightarrow \nu_\mu)$  the fraction that transformed into  $\nu_\mu$ . Since these fractions are oscillatory functions of time, the composition along the beam varies sinusoidally as shown in Figure 1.4. The  $\nu_1$  and  $\nu_2$  states in the superposition that was  $\nu_e$  have equal momenta; but because the masses are not equal, each eigenstate picks up a different phase factor as it travels. Had we assumed that the *energies* are equal then the travelling eigenstates will pick up different phase factors from different  $p$ 's in  $\exp(-ipx)$ . Thus oscillation results from the interference between these eigenstates of *unequal* masses; it will not occur if the masses are degenerate or if there is no mixing between the two eigenstates ( $\theta = 0$ ).

Here we have considered only two-neutrino mixing. The three-neutrino case has three more parameters, but the qualitative features are similar. Oscillations in matter are much more complicated and will be treated in Chapter 2.

A familiar analog in which the propagation eigenstates are different from the detection eigenstates is optical rotation[15]. Light is described as a superposition of two orthogonal plane polarized states when its direction of polarization is measured with a sheet of polaroid. Malus' Law for example, which describes the detection of plane polarized light, is derived by decomposing the incident beam into components parallel and perpendicular to the transmission axis of the polaroid. But when light propagates, it is described as a superposition of orthogonal right- and left-circularly polarized



Figure 1.4: The composition along the beam varies sinusoidally with distance  $l$  from the source.

states. In an optically active medium (different refractive indices for left- and right-circular light), the two states pick up different phases as they travel. And the direction of polarization is found to have rotated when one reverts to the basis of plane polarized states.

## Detecting Neutrino Oscillations

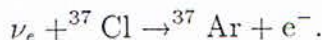
The clearest proof of oscillation is observing a sinusoidal time (or length) variation in the composition of a current of neutrinos. But whether this is possible depends crucially on the oscillation length  $l_v$ . One can work only with conveniently available lengths  $l$  such as the length of one's laboratory or the distance from the Sun (a powerful neutrino source) to the Earth. Suppose  $l$  is the distance from a neutrino source to a detector, whose size is small compared to  $l$ . If in (1.12) and (1.13)  $l_v \gg l$ , then oscillations have not yet started at the detector. If  $l_v \ll l$ , then oscillations may be too rapid to be observed. For if the size of the detector is large compared to  $l_v$ , the neutrinos would have oscillated many times while going through the detector. There is only an average effect  $\langle \sin^2(\pi l/l_v) \rangle \sim 1/2$ , and the fraction of each species measured will be constant. Only when  $l_v \sim l$  can any depletion or enrichment of a neutrino flavor be readily observed.

Experiments to detect neutrino oscillation include measurements of the neutrino flux produced by specific reactor reactions and detecting day-night

or seasonal variations in the solar neutrino flux. (One such experiment will be described in Chapter 2). No conclusive evidence for oscillation has yet been found, although certain combination of  $\Delta m^2$  and  $\theta$  values has been ruled out by these experiments[16].

## 1.5 The Solar Neutrino Problem

In the Standard Solar Model (SSM)  $\nu_e$ 's are produced abundantly in a series of fusion reactions in the solar core. The principal reactions, neutrino energies and neutrino fluxes through the Earth are given in Figure 1.5 reproduced from reference [15]. The total flux is enormous and is predominated ( $> 90\%$ ) by neutrinos produced in the basic pp reaction. Their low energies make them very difficult to detect. Until recently there has only been one experiment to observe solar neutrinos, which began in 1970 in a detector down in the Homestake Gold Mine[17]. A tank of  $4 \times 10^5$  liters of  $C_2Cl_4$  shielded by 1.5km of earth captures neutrinos through the process



This reaction has a threshold energy of 0.81 MeV and is optimally sensitive to the high-energy neutrinos produced in the  ${}^8\text{B}$  reaction, which contributes  $\sim 80\%$  of the capture rate[21]. The pp neutrinos are not observed, while the rest contribute  $\sim 20\%$ . The capture rate is determined by counting the number of  ${}^{37}\text{Ar}$  produced. The average rate (Ar atoms/day) measured in the period 1970–86 is only 27% of the value predicted by the standard solar model:

$$\text{capture rate} = \begin{cases} 2.1 \pm 0.3 & \text{SNU (Homestake 1970–86)} \\ 5.3 - 10.5 & \text{SNU (SSM)} \end{cases}$$

Here SNU = Solar Neutrino Unit =  $10^{-36}$  interactions/target atom/s; 5.3–10.5 SNU is also expressed as  $7.9 \pm 2.6(3\sigma)$  SNU[18]. The range quoted for the SSM values accounts for all possible initial conditions in the evolution of the Sun that could have led to its present luminosity and other properties. Although the Homestake value has fluctuated occasionally (eg. highs  $4.2 \pm 0.8$ [19] SNU (1986–88) and  $\sim 5.1$  SNU (1977–78)), it has remained consistently below the theoretical value for 18 years. This deficiency is known as the Solar Neutrino Problem.



Figure 1.5: Standard model solar neutrino fluxes; continuum sources in units  $\text{cm}^2\text{sec}^{-1}\text{Mev}^{-1}$ , line sources in  $\text{cm}^{-2}\text{sec}^{-1}$ .

The flux was also measured recently by the Kamiokande-II reactor[20], which detects neutrinos through neutrino-electron scattering  $\nu_e e^- \rightarrow \nu_e e^-$ . This process has a threshold of  $\sim 9\text{MeV}$  and is therefore sensitive only to the  ${}^8\text{B}$  flux. The result is about 46% of value predicted by the SSM; it is consistent with the Homestake value after correcting for the unobserved lower energy fluxes.

## Possible Solutions

There are two candidates:

1. The standard solar model, or at least the portion that implied the neutrino spectrum to which the Homestake detector is sensitive, is wrong. But because the SSM must simultaneously account for many observed properties, it is difficult to adjust it to obtain a lower  ${}^8\text{B}$  flux without adding a lot of new physics.
2. The neutrinos transform—decay, precess, oscillate—along the way to Earth. Neutrino decay over 1 A.U. has been ruled out by the survival of the neutrinos from SN1987a (see section 1.3). Neutrino spin precession occurs when a left-handed neutrino precesses into a right-handed neutrino in the presence of an external magnetic field. Only left-handed neutrinos are involved in weak interactions; they are the ones produced in, and detected by, nuclear reactions. Right-handed neutrinos, if they exist, do not interact. If some of the left-handed  $\nu_e$ 's produced in the solar core change their handedness as they travel through the solar magnetic field, they will not be observed by the Homestake detector. But for this to happen the neutrino must have a large magnetic moment, which seems unreasonable on account of present theories[15]. There are also other complications, and the sentiment is that spin precession is unlikely to occur. So we are left with neutrino oscillation as a plausible resolution of the problem.

Vacuum oscillations may be the answer, but only if the mixing angle  $\theta$  is large. A reduction to about half the  $\nu_e$  flux to explain the deficiency requires  $\theta \geq \pi/8$  (cf. (1.12) and (1.13) where  $\sin^2 2\theta \sim 1/2$  implies  $\theta \sim \pi/8$ ). But such large values for  $\theta$  seem unreasonable within theories requiring a non-zero neutrino mass. Fortunately when oscillations occur in matter, a mechanism exists that efficiently converts neutrinos of one flavor to

another when certain conditions are met. This is the Mikheyev-Smirnov-Wolfenstein (MSW) effect to be discussed in Chapter 2. For the solar neutrinos the conversion may occur while they travel from the core where they are produced to the surface. And it may occur even for neutrino masses of less than  $10^{-2}\text{eV}$  and for  $\theta < 10^{-2}$ [23]. So matter oscillations together with the MSW effect offer a likely solution to the solar neutrino problem.

# Chapter 2

## MATTER OSCILLATIONS

### 2.1 Matter Oscillations

#### Propagation in Vacuum

If its spin structure is neglected, the neutrino propagates, or develops in time (since length = time for a particle that travels at close to  $c$ ), according to the Klein-Gordon equation

$$(\nabla^2 - m^2)|\nu\rangle = \frac{\partial^2}{\partial t^2}|\nu\rangle. \quad (2.1)$$

This equation, which is the relativistic analog of the Schrodinger's equation, is obtained from the relation  $E^2 = p^2 + m^2$  with the substitutions  $E \rightarrow i\partial/\partial t$  and  $p \rightarrow -i\nabla$ . The mass eigenstates satisfy (2.1) since they are also eigenstates of energy and momentum. It is in this sense that the neutrino propagates in vacuum in its mass eigenstates. For  $n$  neutrino flavors, we can write the propagation equations in the mass basis  $|\nu_i\rangle$  as a single matrix equation

$$(\delta_{ij}\nabla^2 - m_{ij}^2)|\nu_j(t)\rangle = \frac{\partial^2}{\partial t^2}|\nu_i(t)\rangle \quad (2.2)$$

where  $i, j = 1 \dots n$  and  $m_{ij}^2$  is a  $n \times n$  diagonal matrix consisting of the mass eigenvalues squared. Assuming relativistic neutrinos from a coherent source—i.e. equal  $p_i$ 's, (2.2) can be reduced to a first-order equation with the substitution

$$|\nu_i(t)\rangle = \exp(-iE_it)|\nu_i\rangle \simeq \exp(-ipt)|\nu_i\rangle.$$



So we obtain<sup>1</sup>

$$(p_{ij}^2 + m_{ij}^2)|\nu_j(t)\rangle = ip \frac{\partial}{\partial t} |\nu_i(t)\rangle. \quad (2.3)$$

where  $p_{ij}^2$  is diagonal and consists of squared momentum eigenvalues. Note that  $\nabla^2 |\nu_i(t)\rangle = \exp(-ipt) \nabla^2 |\nu_i\rangle = -p^2 |\nu_i(t)\rangle$ . The combination  $(p_{ij}^2 + m_{ij}^2)$  is known as the propagation matrix. Since  $p_{ij}^2$  is proportional to the identity matrix, it contributes the same phase factor to all the propagation eigenstates when (2.3) is integrated to solve for them. If only neutrino oscillation, which comes from interference between different propagation eigenstates, is to be considered, we may neglect the  $p_{ij}^2$  term and write

$$m_{ij}^2 |\nu_j(t)\rangle = ip \frac{\partial}{\partial t} |\nu_i(t)\rangle. \quad (2.4)$$

A propagation equation in the flavor basis can be obtained from (2.4) by means of a similarity transformation

$$(UM^2U^\dagger)U|\nu\rangle = ip \frac{\partial}{\partial t} U|\nu\rangle \quad (2.5)$$

where  $U$  is the unitary matrix in (1.3),  $M^2 = m_{ij}^2$  and  $|\nu\rangle$  is understood to be a column matrix of wave-functions. The combination  $W = UM^2U^\dagger$  is the propagation matrix for the weak-interaction eigenstates  $|\nu_\alpha\rangle = U_{\alpha j} |\nu_j\rangle$ . (Latin and Greek subscripts respectively label mass and weak-interaction eigenstates). Considering only two flavors, (2.5) appears explicitly as

$$ip \frac{\partial}{\partial t} \begin{pmatrix} \nu_e \\ \nu_\mu \end{pmatrix} = \begin{pmatrix} m_1^2 \cos^2 \theta + m_2^2 \sin^2 \theta & -(m_2^2 - m_1^2) \sin \theta \cos \theta \\ -(m_2^2 - m_1^2) \sin \theta \cos \theta & m_1^2 \sin^2 \theta + m_2^2 \cos^2 \theta \end{pmatrix} \begin{pmatrix} \nu_e \\ \nu_\mu \end{pmatrix}. \quad (2.6)$$

This propagation matrix is diagonal only when the masses are degenerate or when the vacuum mixing angle  $\theta$  is zero. In the last case it reduces to  $M^2$ ; and each decoupled weak-interaction eigenstate separately satisfies its own Klein-Gordon equation and is therefore a propagation eigenstate.

---

<sup>1</sup>The first-order equation has only one solution, whereas the second-order equation (2.1) has two corresponding to waves travelling in opposite directions. We are disregarding the reflected solution—see [23].

## Propagation in Matter

We have hitherto considered only vacuum propagation. Neutrinos travelling in matter scatter from electrons or nuclei. The elastic scattering  $\nu_e e^- \rightarrow \nu_e e^-$  via the charged current interaction generates a refractive index  $n$  (i.e. the interaction accelerates the neutrino) given by[15]

$$\Delta n = n - 1 = -\sqrt{2}G_F\rho/E \quad (2.7)$$

where  $G_F$  is the weak-coupling constant,  $\rho$  the number density of electrons in the medium and  $E$  the energy of the neutrino. If  $\Delta n \neq 0$ , there is a path difference relative to a neutrino travelling in free space of  $\Delta n L$ , where  $L$  is the distance travelled, which leads to an extra propagation phase factor<sup>2</sup>  $\exp(iE\Delta n L)$ . Neutrino scattering via the neutral current interaction gives refractive indices that are the same for all neutrino species. It merely gives to all states a common phase that may be ignored.

The mixing amplitudes in (2.6), i.e. the elements in the propagation matrix, determine the relative phases of the interfering eigenstates. Since only the phase of the  $\nu_e$  state is modified in matter, the matter propagation equation in the weak interaction basis has the form

$$ip \frac{\partial}{\partial t} \begin{pmatrix} \nu_e \\ \nu_\mu \end{pmatrix} = \left[ (UM^2U^\dagger) + \begin{pmatrix} \zeta & 0 \\ 0 & 0 \end{pmatrix} \right] \begin{pmatrix} \nu_e \\ \nu_\mu \end{pmatrix}$$

where  $\zeta$  depends on  $E$  and  $\rho$ . Actually the Klein-Gordon equation is not applicable here since the neutrino spin figures in matter. It can be shown[15] that the correct propagation equation derived from the Dirac equation is

$$2ip \frac{\partial}{\partial t} \begin{pmatrix} \nu_e \\ \nu_\mu \end{pmatrix} = \begin{pmatrix} m_1^2 \cos^2 \theta + m_2^2 \sin^2 \theta + 2\sqrt{2}G_F E \rho & -(m_2^2 - m_1^2) \sin \theta \cos \theta \\ -(m_2^2 - m_1^2) \sin \theta \cos \theta & m_1^2 \sin^2 \theta + m_2^2 \cos^2 \theta \end{pmatrix} \begin{pmatrix} \nu_e \\ \nu_\mu \end{pmatrix} \quad (2.8)$$

This equation resembles the Klein-Gordon equation except for a factor of 2.

To solve (2.8) we first obtain the eigenvalues  $M_{1,2}^2$  of the propagation matrix by solving the determinant equation

$$\begin{vmatrix} m_1^2 \cos^2 \theta + m_2^2 \sin^2 \theta + 2\sqrt{2}G_F E \rho - M_{1,2}^2 & -(m_2^2 - m_1^2) \sin \theta \cos \theta \\ -(m_2^2 - m_1^2) \sin \theta \cos \theta & m_1^2 \sin^2 \theta + m_2^2 \cos^2 \theta - M_{1,2}^2 \end{vmatrix} = 0.$$

<sup>2</sup>The phase difference is  $\phi = 2\pi(L/\lambda_{medium} - L/\lambda_{free})$ , where  $\lambda_{medium} = \lambda_{free}/n$ . So  $\phi = k_{free}\Delta n L = E\Delta n L$ , since  $L = t$  and  $E = \omega$ .

Writing  $\delta m^2 = m_2^2 - m_1^2$ , the answer is

$$M_{1,2}^2 = \frac{1}{2} \{ 2\sqrt{2}G_F E\rho + m_1^2 + m_2^2 \mp [(2\sqrt{2}G_F E\rho - \delta m^2 \cos 2\theta)^2 + (\delta m^2 \sin 2\theta)^2]^{\frac{1}{2}} \}, \quad (2.9)$$

$M_{1,2}^2$  are also the elements of the diagonalized propagation matrix obtained from (2.8) via a similarity transformation. That is, if  $W_1$  is the nondiagonal propagation matrix in (2.8) and we use the transformation

$$U_m = \begin{pmatrix} \cos \theta_m & -\sin \theta_m \\ \sin \theta_m & \cos \theta_m \end{pmatrix}$$

where

$$U_m^\dagger W_1 U_m = \begin{pmatrix} M_1^2 & 0 \\ 0 & M_2^2 \end{pmatrix},$$

then by multiplying both sides of (2.8) by  $U_m^\dagger$  and inserting  $U_m U_m^\dagger = I$  we obtain

$$2ip \frac{\partial}{\partial t} U_m^\dagger \begin{pmatrix} \nu_e \\ \nu_\mu \end{pmatrix} = U_m^\dagger W_1 U_m U_m^\dagger \begin{pmatrix} \nu_e \\ \nu_\mu \end{pmatrix}. \quad (2.10)$$

Now recognizing that

$$\begin{pmatrix} \nu_{1m} \\ \nu_{2m} \end{pmatrix} = U_m^\dagger \begin{pmatrix} \nu_e \\ \nu_\mu \end{pmatrix}. \quad (2.11)$$

where  $|\nu_{1m,2m}\rangle$  are *matter* eigenstates, we obtain the diagonal form

$$2ip \frac{\partial}{\partial t} \begin{pmatrix} \nu_{1m} \\ \nu_{2m} \end{pmatrix} = \begin{pmatrix} M_1^2 & 0 \\ 0 & M_2^2 \end{pmatrix} \begin{pmatrix} \nu_{1m} \\ \nu_{2m} \end{pmatrix}. \quad (2.12)$$

From (2.10) a relation between the *matter* mixing angle  $\theta_m$  and the vacuum angle  $\theta$  can be obtained:

$$\tan 2\theta_m = \frac{\tan 2\theta}{1 - 2\sqrt{2}G_F E\rho / \delta m^2 \cos 2\theta}. \quad (2.13)$$

These angles are conventionally taken to be positive.

From (2.13) we note the following



1. No vacuum mixing ( $\theta = 0$ ) implies no matter mixing.
2. If  $G_F E \rho \ll \delta m^2 \cos^2 \theta$ , the medium has negligible effect and oscillations are as those in vacuum.
3. If  $G_F E \rho \gg \delta m^2 \cos^2 \theta$ , then  $\theta_m \simeq 0$  and there will be little or no oscillation.
4. If  $G_F E \rho = \delta m^2 \cos^2 \theta$ , then  $\theta_m = \pi/4$  and there will be maximum mixing (ie. equal portions of  $\nu_1$  and  $\nu_2$ ). This is called resonance, and the value of  $\rho$  at which this happens is the resonant density. Oscillations may or may not be pronounced depending on  $\delta m^2$ .

## Varying Density

The propagation equation in a medium of varying density remains as (2.8) except that  $\theta$  and  $\rho$  are now functions of position. Using (2.8) and (2.11) we write it as

$$\begin{aligned}
 2ip \frac{\partial}{\partial t} \begin{pmatrix} \nu_e \\ \nu_\mu \end{pmatrix} &= U_m \begin{pmatrix} M_1^2 & 0 \\ 0 & M_2^2 \end{pmatrix} U_m^\dagger \begin{pmatrix} \nu_e \\ \nu_\mu \end{pmatrix} \\
 &= U_m \begin{pmatrix} M_1^2 & 0 \\ 0 & M_2^2 \end{pmatrix} \begin{pmatrix} \nu_{1m} \\ \nu_{2m} \end{pmatrix}.
 \end{aligned} \tag{2.14}$$

We might as well equate  $\partial/\partial t$  with  $\partial/\partial l$  since the neutrino travels at close to the speed of light. So

$$U_m^\dagger i \frac{\partial}{\partial l} \begin{pmatrix} \nu_e \\ \nu_\mu \end{pmatrix} = \frac{1}{2p} \begin{pmatrix} M_1^2 & 0 \\ 0 & M_2^2 \end{pmatrix} \begin{pmatrix} \nu_{1m} \\ \nu_{2m} \end{pmatrix} \tag{2.15}$$

and because  $U_m^\dagger$  is now  $l$ -dependent we have

$$\begin{aligned}
 i \left\{ \frac{\partial}{\partial l} \left[ U_m^\dagger \begin{pmatrix} \nu_e \\ \nu_\mu \end{pmatrix} \right] - \left( \frac{\partial}{\partial l} U_m^\dagger \right) \begin{pmatrix} \nu_e \\ \nu_\mu \end{pmatrix} \right\} \\
 = \frac{1}{2p} \begin{pmatrix} M_1^2 & 0 \\ 0 & M_2^2 \end{pmatrix} \begin{pmatrix} \nu_{1m} \\ \nu_{2m} \end{pmatrix}
 \end{aligned} \tag{2.16}$$

Note that the matter eigenstates are *local*, i.e. position dependent. We have

$$i \frac{\partial}{\partial l} \begin{pmatrix} \nu_{1m} \\ \nu_{2m} \end{pmatrix} = \frac{1}{2p} \left[ \begin{pmatrix} M_1^2 & 0 \\ 0 & M_2^2 \end{pmatrix} + i \frac{\partial}{\partial l} (U_m^\dagger) U_m \right] \begin{pmatrix} \nu_{1m} \\ \nu_{2m} \end{pmatrix} \quad (2.17)$$

It is easily shown that

$$i \frac{\partial}{\partial l} (U_m^\dagger) U_m = \begin{pmatrix} 0 & -i \frac{\partial \theta_m}{\partial l} \\ i \frac{\partial \theta_m}{\partial l} & 0 \end{pmatrix}$$

with

$$i \frac{\partial \theta_m}{\partial l} = i 2 \sqrt{2} G_F p^2 \sin 2\theta \frac{\delta m^2}{(\delta M^2)^2} \frac{d\rho}{dl}.$$

The propagation equation now has the form

$$i \frac{\partial}{\partial l} \begin{pmatrix} \nu_{1m} \\ \nu_{2m} \end{pmatrix} = \frac{1}{2p} \begin{pmatrix} M_1^2 & -i \frac{\partial \theta_m}{\partial l} \\ i \frac{\partial \theta_m}{\partial l} & M_2^2 \end{pmatrix} \begin{pmatrix} \nu_{1m} \\ \nu_{2m} \end{pmatrix}. \quad (2.18)$$

This equation can be integrated numerically along the neutrino trajectory for any given electron density profile  $\rho(l)$ . The off-diagonal element in the propagation matrix in (2.18) can be regarded as a perturbation that mixes the matter eigenstates. It can be shown that if  $\rho(l)$  varies so slowly ( $\partial\rho/\partial l \ll 1$ ) that  $\partial\theta_m/\partial l \ll |\delta M^2|$ , i.e. the characteristic length ('rise time') of the perturbation is small compared to  $1/\omega$  where  $\omega$  are frequencies associated with energies in the system, then the *adiabatic theorem*[24] applies and the ordering of the local eigenstates is preserved throughout the perturbation. A neutrino that starts out before the perturbation in a local upper (lower) matter eigenstate remains in a local upper (lower) state after the perturbation. The local states are of course different since the perturbation changes the eigenvalues as the neutrino travels. Thus if  $m_0, M_0$ , where  $m_0 < M_0$ , are the two mass eigenvalues before the perturbation, and the neutrino is in the state  $|\nu_{M_0}\rangle$  (the higher mass state), then it will emerge from the perturbation in the state  $|\nu_M\rangle$  where  $M$  is the larger of the two new eigenvalues  $M$  and  $m$ . Similarly a  $|\nu_{m_0}\rangle$  will emerge as a  $|\nu_m\rangle$ .

## MSW Effect

Mikheyev, Smirnov and Wolfenstein[25] discovered that a neutrino propagating adiabatically through a medium of varying density could transform from a  $|\nu_e\rangle$  to a  $|\nu_\mu\rangle$  if certain conditions are met. The mechanism is the following: Suppose a  $|\nu_e\rangle$  is produced in the solar core, where the electron density is so high that

$$\rho \gg \frac{\delta m^2 \cos 2\theta}{2\sqrt{2}G_F E}. \quad (2.19)$$

Then (2.13) shows that  $\tan 2\theta_m$  is small and negative, i.e.  $\theta_m \simeq \pi/2$ . Except for a phase factor, the  $|\nu_e\rangle$  is now almost a pure local  $|\nu_{2m}\rangle$  since the mixing equation is

$$\begin{pmatrix} \nu_e \\ \nu_\mu \end{pmatrix} = \begin{pmatrix} \cos \theta_m & -\sin \theta_m \\ \sin \theta_m & \cos \theta_m \end{pmatrix} \begin{pmatrix} \nu_{1m} \\ \nu_{2m} \end{pmatrix} \simeq \begin{pmatrix} 0 & -1 \\ 1 & 0 \end{pmatrix} \begin{pmatrix} \nu_{1m} \\ \nu_{2m} \end{pmatrix}.$$

Suppose  $\rho$  decreases slowly enough to preserve the adiabatic condition. (The drop in density with distance from the core is well described by an exponential). Then the neutrino always stays in the lower local eigenstate  $|\nu_{2m}\rangle$  as it travels from the solar core into interplanetary space. Since in vacuum the mixing angle  $\theta$  is expected to be small, the mixing equation gives

$$\begin{pmatrix} \nu_e \\ \nu_\mu \end{pmatrix} \simeq \begin{pmatrix} 1 & 0 \\ 0 & 1 \end{pmatrix} \begin{pmatrix} \nu_{1m} \\ \nu_{2m} \end{pmatrix}$$

Now the lower matter eigenstate  $|\nu_{2m}\rangle$  corresponds to almost a pure  $|\nu_\mu\rangle$ . Hence the  $\nu_e$  had been converted into a  $\nu_\mu$ .

A level crossing diagram will nicely illustrate the conversion process. But we will not belabor the treatment since such diagrams are presented in practically every paper on the subject. Many detailed calculations have also been performed to determine the parameters  $\delta m^2$  and  $\theta$  required for a MSW effect significant enough to suppress 2/3 of the  $\nu_e$  flux from the Sun. In the above parametrization for example, a  $\delta m^2$  of  $\sim 10^{-4}$  eV<sup>2</sup> would satisfy (2.19), given a core density of  $\sim 10^{31}\text{m}^{-3}$ . A more refined analysis must sustain the requirements of the adiabatic approximation—which imposes a range of values for  $\theta$ —and agree with the Homestake flux measurement; but a range of values of  $10^{-4}$  eV<sup>2</sup> or smaller for  $\delta m^2$  would still emerge nonetheless[15].



## Chapter 3

# $\bar{\nu}_e d \rightarrow n n e^+$ CROSS-SECTION

### 3.1 Deuterium Reactions

Neutrino reactions in deuterium, including the neutral current ( $Z^0$  exchange) reaction  $\nu + {}^2\text{H} \rightarrow \text{p} + \text{n} + \nu$  and the charged current ( $W^+$  exchange) reactions  $\bar{\nu} + {}^2\text{H} \rightarrow \text{n} + \text{n} + e^+$  and  $\bar{\nu} + {}^2\text{H} \rightarrow \text{p} + \text{p} + e^-$ , are particularly useful to study because (1) the deuteron is the simplest of many-nucleon nuclei; and (2) many experiments to detect neutrino oscillation involve these deuterium processes. Experimental results[28] (1981) for the cross-sections  $\langle \sigma(\bar{\nu}_e {}^2\text{H} \rightarrow n n e^+) \rangle$  and  $\langle \sigma(\bar{\nu}_e {}^2\text{H} \rightarrow n p \bar{\nu}_e) \rangle$  at low neutrino energies were found to be in agreement with theoretical calculations based on the Weinberg-Salaam model. These positive measurements have motivated several experiments using these reactions to measure neutrino fluxes.

### Neutrino Flux Measurements

One such experiment[28] (1980) which engendered the claim that evidence for neutrino oscillations has been found is the following: A tank of  $\text{D}_2\text{O}$  captures  $\bar{\nu}_e$ 's from a fission reactor situated 11.2m away via both the charge current (CC) process

$$\bar{\nu}_e + d \rightarrow e^+ + n + n$$

and the neutral current (NC) process

$$\bar{\nu}_e + d \rightarrow \bar{\nu}_e + p + n.$$

The CC and NC cross-sections were measured and a comparison made with theoretical values calculated assuming a zero-mass neutrino (i.e. no oscillations possible). The motivation behind is that given the low energy neutrinos from the reactor, a  $\bar{\nu}_\mu$  or  $\bar{\nu}_\tau$  in their midst that has come about because of oscillations would not have enough energy to cause the CC reactions

$$\begin{aligned}\bar{\nu}_\mu + d &\rightarrow \mu^+ + n + n \\ \bar{\nu}_\tau + d &\rightarrow \tau^+ + n + n\end{aligned}$$

since the energy supplied by the neutrino is below the threshold needed to create the  $\mu^+$  and  $\tau^+$ . As a result the measured CC cross-section *in the presence of oscillations* will be smaller than the theoretical value. However, the  $\bar{\nu}_\mu$  or  $\bar{\nu}_\tau$  could still cause the NC reactions

$$\begin{aligned}\bar{\nu}_\mu + d &\rightarrow \bar{\nu}_\mu + p + n \\ \bar{\nu}_\tau + d &\rightarrow \bar{\nu}_\tau + p + n\end{aligned}$$

since no new particles are created. And the NC cross-sections for all three flavors are equal which means that the measured NC cross-section will remain the same as the theoretical value even in the presence of oscillations. Therefore if neutrinos oscillate, we would have

$$R = \frac{\sigma(CC)_{ex}}{\sigma(NC)_{ex}} < \frac{\sigma(CC)_{th}}{\sigma(NC)_{th}}.$$

Indeed the experimenters found that

$$R \simeq (0.4 \pm 0.2) \frac{\sigma(CC)_{th}}{\sigma(NC)_{th}}$$

and since  $\sigma(NC)_{ex} = \sigma(NC)_{th}$ , this implies that  $\sigma(CC)_{ex} < \sigma(CC)_{th}$ . So a significant new effect attributable to neutrino oscillation seems to be present. Unfortunately this result has been overrun by criticisms of both the experimental procedure and the theoretical groundwork. (For example  $\sigma(CC)_{th}$  may not have been calculated properly). But the idea of comparing CC and NC reaction rates is useful and has been applied in another experiment that we will now describe.

This experiment, proposed to resolve the solar neutrino problem, uses 1 kiloton of  $D_2O$  down in a mine in Sudbury, Ontario, to capture neutrinos produced in the  ${}^8B$  reaction in the Sun through both the flavor-specific reaction

$$\nu_e + {}^2H \rightarrow p + p + e^- \quad (3.1)$$

and the flavor-indifferent reaction (where  $x = e, \mu, \text{ or } \tau$ )

$$\nu_x + {}^2H \rightarrow \nu_x + p + n. \quad (3.2)$$

As noted the last reaction has the same cross-section for all three types of neutrinos. Hence by comparing the  $\nu_e$  flux measured with (3.1) and the total flux measured with (3.2) one could confirm  $\nu_e$  flux depletion independent of the standard solar model. A depletion would be indicative of neutrino transformation of some sort.

In this chapter we will study the reaction  $\bar{\nu}_e {}^2H \rightarrow nne^+$  and calculate the reaction rate for the process in which a single neutrino engages the deuteron. This is equal to the cross-section (the experimentally relevant quantity) for unit incident flux. This reaction is easier to study than (3.1) because there is no electromagnetic interaction between the two final state neutrons. The cross-sections for both reactions are exactly the same to order  $G_F^2$ [26], where  $G_F$  is the weak-coupling constant. (That is, the cross-sections will be equal in the 1st-order perturbation theory approximation that we will be using to calculate them). The cross-section has been calculated by Weneser[27] (1957—before the discovery of the antineutrino) and improved upon by Mintz[26] in a series of articles (1974–1981). The most detailed calculation to date was done by Ying[29] et al (1989).

## 3.2 $\bar{\nu}_e d \rightarrow nne^+$ Cross Section

### Previous Work

If  $J_{inc}$  is the incident flux (particles/area/time) and  $dN$  the number of *product* particles to be found in a solid angle  $d\Omega$  per unit time, the differential cross-section  $\sigma$  is defined as

$$\sigma d\Omega = \frac{dN}{J_{inc}}. \quad (3.3)$$



In the reaction  $\bar{\nu}_e d \rightarrow n n e^+$  in which a single incident neutrino disintegrates the deuteron,  $J_{inc}$  is just  $c/V$ , where  $V$  is volume of the ‘box’ in which our wavefunctions are normalized, and  $dN$  is the transition probability rate between incident and product states. The Golden Rule from 1st-order time-dependent perturbation theory gives

$$N = \frac{2\pi}{\hbar} |\langle \Phi_f | H_{int} | \Phi_i \rangle|^2 \delta(E_f - E_i). \quad (3.4)$$

where  $|\Phi_i\rangle = |\bar{\nu}_e d\rangle$  and  $\langle \Phi_f| = \langle n n e^+|$  and  $H_{int}$  is the weak-interaction hamiltonian.

A cross-section calculation thus rests upon the evaluation of the matrix element  $\langle \Phi_f | H_{int} | \Phi_i \rangle$ . For our problem the older approach by Weneser[27] is to evaluate an integral of the form

$$\int \Psi_f^*(\mathbf{r}_1, \zeta_1; \mathbf{r}_2, \zeta_2) H_{int} \Psi_i(\mathbf{r}_1, \zeta_1; \mathbf{r}_2, \zeta_2) d\tau_1 d\tau_2 \quad (3.5)$$

where  $\Psi_i$  is the deuteron ground state wavefunction and  $\Psi_f$  the wavefunction for the two final-state neutrons. The nucleon space and spin coordinates  $\mathbf{r}_i, \zeta_i$  are simultaneously for the proton and the neutron before the interaction *and* the two neutrons after the interaction. This amounts to assuming the neutrino interacts only with the proton in the deuterium nucleus and changes it into a neutron. The integral involving the neutrino and positron wavefunctions decouples from the one involving nuclear wavefunctions in the matrix element and is easy to calculate as we will see later.

To evaluate (3.5) we first note that the neutron and proton are so loosely bound that there is only one deuteron bound state. This ground state is composed mainly of  $^3S$  with the nucleons having parallel spins. (In the notation  $^{2s+1}S$ ,  $^3S$  corresponds to two nucleons with parallel spins ( $s = 1/2 + 1/2$ ) and  $^1S$  corresponds to opposite spins). Thus the final state will also be  $^1S$  and  $^3S$  mostly. The spins of the final-state neutrons cannot be parallel because of the Pauli exclusion principle; so the final state is only  $^1S$ . The spin-flip is effected by the weak-interaction; and in an approximation good to within 10% of the final result the  $H_{int}$  operator is taken to have the sole effect of flipping the spin of one of the nucleons. Thus the matrix element is simply between a two-neutron  $^1S$  state and the  $^3S$  deuteron ground state (with  $H_{int} = 1$ ). The wavefunctions in a judicious choice of coordinates are functions only of the nucleons’ relative separation and spins.

The angular integrations are straightforward and it remains to evaluate

$$\int \phi_S(r) \phi_g(r) r^2 dr$$

where  $r$  is the relative separation  $|\mathbf{r}_1 - \mathbf{r}_2|$  and  $\phi_S$  and  $\phi_g$  are the two-neutron and the deuteron wavefunctions respectively.

Although the above method neatly takes care of the exclusion requirement of the neutrons, it involves the use of nuclear wavefunctions  $\phi_S, \phi_g$  which are not generally well-known. And the cross-section sometimes depend sensitively on these wavefunctions. The other approach, which does not involve nuclear wavefunctions, is to treat the deuteron as a single elementary particle that is free up to the point the neutrino (also a free particle) impinges on it. This is the elementary-particle model where all interacting particles are regarded as plane-wave states. The range of the weak interaction is short enough for this model to be valid in this problem. This approach is taken in the calculation by Mintz[26], an outline of which follows.

In the modern theory of weak-interactions the transition matrix element is written as

$$M(\bar{\nu}_e d \rightarrow n n e^+) = \frac{G_F}{\sqrt{2}} \cos \theta_C \langle n n | J_\lambda^\dagger | d \rangle \langle e^+ | \bar{\psi} \gamma^\lambda (1 - \gamma_5) \psi | \bar{\nu}_e \rangle \quad (3.6)$$

where  $G_F$  ( $\simeq 10^{-5}/m_p^2$ ) is the weak-coupling constant and  $\theta_C$  ( $\cos \theta_C = 0.98$ ) is the Cabibbo angle. The interaction may be thought of as between a weak hadron current  $J_\lambda^\dagger$  (of the deuteron and neutrons) and a weak lepton current  $j^\lambda = \bar{\psi} \gamma^\lambda (1 - \gamma_5) \psi$  (of the antineutrino and positron) mediated by a  $W^+$  vector boson. Replacing the fermion states with Dirac spinors  $\bar{u}, \bar{v}$  and boson states with polarization vectors  $\epsilon$ , and collecting all constants and spinor normalization factors into  $\eta$ , we have

$$M(\bar{\nu}_e d \rightarrow n n e^+) = \eta \bar{u}_\alpha \bar{u}_\beta J_\lambda^\dagger \epsilon \bar{v}_{\bar{\nu}_e} \gamma^\lambda (1 - \gamma_5) \bar{v}_{e^+}.$$

Here  $\alpha$  and  $\beta$  labels the two neutrons. To account for their Pauli exclusion, the hadron current must have the form

$$\langle n n | J_\lambda^\dagger | d \rangle = \bar{u}_\alpha \bar{u}_\beta C_\lambda^\nu(p_1, p_2, d)_{\alpha\beta} \epsilon_\nu$$

where the 4x4 matrix  $C_\lambda^\nu(p_1, p_2, d)_{\alpha\beta}$  is a function of the neutrons' 4-momenta  $p_1, p_2$  and the deuteron 4-momentum  $d$  and is exchange antisymmetric:

$$C_\mu^\nu(p_1, p_2, d)_{\alpha\beta} = -C_\mu^\nu(p_2, p_1, d)_{\beta\alpha}.$$



This ensures that the squared matrix element remains the same under the exchange  $p_1 \leftrightarrow p_2, \alpha \leftrightarrow \beta$ . (Note that  $\alpha$  and  $\beta$  are contracted spinor indices).

It remains to determine the form of the Lorentz 4-vector  $C_\mu^\nu(p_1, p_2, d)_{\alpha\beta}\epsilon_\nu$  which must be expressible as a function of the 4-momenta of the interacting particles and bilinear covariants constructed from  $\gamma$  matrices. Generally

$$C_\mu^\nu(p_1, p_2, d)_{\alpha\beta}\epsilon_\nu = \sum_i f_i \Gamma_i p_i$$

where  $p_i$  are the 4-momenta of the interacting particles,  $\Gamma_i$  are bilinear covariants and  $f_i$  are scalar functions of *scalars* in the problem, i.e. the dot products  $p_\nu \cdot p_\nu$ ,  $p_n \cdot p_e$ , etc. Mintz has researched painstakingly into the correct form for  $C_\mu^\nu(p_1, p_2, d)$  and has calculated the cross-sections for many neutrino reactions in deuterium. We will not reproduce his work; instead we will calculate the cross-section using a *spectator-neutron* model for the interaction. In this model we assume that only the bound proton in the deuteron participates in the reaction; the bound neutron is merely a spectator. This method still requires the use of nuclear wavefunctions—but only in obtaining the momentum distribution of the bound proton. The calculation presented in detail in the next section is in effect for a process in which a neutrino engages a proton whose momentum is distributed as in the ground state of the deuteron.

## First Approximation

Because of Pauli exclusion, the joint wavefunction of the two neutrons in the final state must be antisymmetrized. But the number of permitted final states into which the neutrons can enter is large enough for failing to antisymmetrize the final-state wavefunction to represent only a small error to the calculated cross-section. So we dispense with antisymmetrization in our first simple-minded model. We also assume that the incoming neutrino interacts only with the proton which is in a bound state of the deuteron. The momentum distribution of the proton is simply the squared modulus of its wavefunction in the momentum representation  $|\phi(\mathbf{p})|^2$ . It is given by the Fourier tranform

$$\phi(\mathbf{q}) = \frac{1}{(2\pi)^{3/2}} \int d^3\mathbf{r} \psi(\mathbf{r}) e^{-i\mathbf{q}\cdot\mathbf{r}} \delta(\mathbf{P} - \mathbf{q}_n - \mathbf{q}_p) \quad (3.7)$$



where  $\psi(\mathbf{r})$  is the deuteron wavefunction in the coordinate representation and  $\mathbf{q}$  is the difference of the neutron and proton momenta  $\mathbf{q}_n - \mathbf{q}_p$ . The neutron plays no part in the interaction and still retains its momentum distribution from the bound state after the interaction.

## Deuterium Ground State

To derive (3.7) we begin with the hamiltonian for the deuteron system

$$H = \frac{\mathbf{q}_n^2}{2m_n} + \frac{\mathbf{q}_p^2}{2m_p} + V(\mathbf{r}_n - \mathbf{r}_p)$$

and use the transformation

$$\begin{aligned} \mathbf{R} &= \frac{m_n \mathbf{r}_n + m_p \mathbf{r}_p}{m_n + m_p} \\ \mathbf{P} &= \mathbf{p}_n + \mathbf{p}_p \\ \mathbf{r} &= \mathbf{r}_n - \mathbf{r}_p \\ \mathbf{q} &= \frac{m_p \mathbf{q}_n - m_n \mathbf{q}_p}{m_n + m_p} \end{aligned} \quad (3.8)$$

to obtain

$$H = \frac{\mathbf{P}^2}{2(m_n + m_p)} + \frac{\mathbf{q}^2}{2\mu} + V(\mathbf{r}). \quad (3.9)$$

The motion of the center of mass is unimportant and we need concern only with the relative hamiltonian

$$H_{rel} = \frac{\mathbf{q}^2}{2\mu} + V(\mathbf{r})$$

whose solution  $\psi(\mathbf{r})$  is related to the solution of (3.9) by

$$\psi(\mathbf{r}_n, \mathbf{r}_p) = \frac{1}{(2\pi)^{3/2}} e^{i\mathbf{P} \cdot \mathbf{R}} \psi(\mathbf{r}) \quad (3.10)$$

To obtain the momentum distribution of the bound proton and neutron, we need to evaluate the Fourier transform

$$\phi(\mathbf{q}_n, \mathbf{q}_p) = \frac{1}{(2\pi)^3} \int d^3\mathbf{r}_n d^3\mathbf{r}_p \psi(\mathbf{r}_n, \mathbf{r}_p) e^{-i\mathbf{q}_n \cdot \mathbf{r}_n} e^{-i\mathbf{q}_p \cdot \mathbf{r}_p}. \quad (3.11)$$

It is easily shown that under the transformation  $(\mathbf{r}_n, \mathbf{r}_p) \rightarrow (\mathbf{r}, \mathbf{R})$

$$\begin{aligned} e^{-i\mathbf{q}_n \cdot \mathbf{r}_n} e^{-i\mathbf{q}_p \cdot \mathbf{r}_p} &= e^{-i(\mathbf{q}_n + \mathbf{q}_p) \cdot \mathbf{R}} e^{-i \frac{(m_n \mathbf{q}_p - m_p \mathbf{q}_n)}{(m_n + m_p)} \cdot \mathbf{r}} \\ &= e^{-i(\mathbf{q}_n + \mathbf{q}_p) \cdot \mathbf{R}} e^{-i\mathbf{q} \cdot \mathbf{r}} \end{aligned}$$

and

$$\begin{aligned} d^3\mathbf{r}_n d^3\mathbf{r}_p &= |J| d^3\mathbf{R} d^3\mathbf{r} \\ &= d^3\mathbf{R} d^3\mathbf{r} \end{aligned}$$

since  $|J| = [(m_n + m_p)/(m_n + m_p)]^3 = 1$ . Then (3.11) can be written as

$$\phi(\mathbf{q}_n, \mathbf{q}_p) = \frac{1}{(2\pi)^{9/2}} \int d^3\mathbf{R} d^3\mathbf{r} e^{i(\mathbf{P} - \mathbf{q}_n - \mathbf{q}_p) \cdot \mathbf{R}} \psi(\mathbf{r}) e^{-i\mathbf{q} \cdot \mathbf{r}} \quad (3.12)$$

where  $\mathbf{q} \simeq (\mathbf{q}_n - \mathbf{q}_p)/2$ . The  $\mathbf{R}$  integration gives a delta function

$$\int d^3\mathbf{R} e^{i(\mathbf{P} - \mathbf{q}_n - \mathbf{q}_p) \cdot \mathbf{R}} = (2\pi)^3 \delta^3(\mathbf{P} - \mathbf{q}_n - \mathbf{q}_p)$$

whence we obtain (3.7).

From experimental data the ground state of the deuteron is found to be composed of 96%  ${}^3S_1$  and 4%  ${}^3D_1$ . The potential that binds the two nucleons is therefore not spherically symmetric; but for simplicity we will neglect the  ${}^3D_1$  admixture and assume a spherically symmetric potential  $V(r)$ . The exact shape of  $V(r)$  is unknown but it may be approximated by a square well of depth  $V_0 \gg \Delta E$  where  $\Delta E$  is the binding energy of the deuteron[33]. (The square well is of course a crude approximation to the potential of the strong force between two nucleons, but it will suffice for our purposes).

Since  $l = 0$  for a S-state wavefunction, the radial equation in spherical coordinates for the ground state of the deuteron is

$$-\frac{1}{2\mu} \frac{\partial}{\partial r} \left[ r^2 \frac{\partial}{\partial r} R(r) \right] + V R(r) = -\Delta E R(r)$$

where  $V = -V_0$  for  $r < a$  and  $V = 0$  for  $r > a$ . Using the standard substitution  $u(r) = rR(r)$ , we obtain

$$-\frac{1}{2\mu} u''(r) + (\Delta E - V_0) u(r) = 0.$$

Figure 3.1: The square well approximation to  $V(r)$ ;  $a$  is the effective radius of the deuteron and  $\Delta E$  its binding energy.

Writing  $K_1 = \sqrt{2\mu(V_0 - \Delta E)}$  and  $K_2 = \sqrt{2\mu\Delta E}$ , the solutions for the two regions are

$$\begin{aligned} r < a: & \quad u(r) = B \sin K_1 r \\ r > a: & \quad u(r) = D e^{-K_2 r}. \end{aligned}$$

The requirement that  $R(0)$  be finite and  $R(\infty)$  be zero precludes a cosine solution for  $r < a$  and a positive exponential for  $r > a$ .

Matching the wavefunctions and their first derivatives at  $r = a$  yields

$$\begin{aligned} B \sin K_1 a &= D e^{-K_2 a} \\ B K_1 \cos K_1 a &= -D K_2 e^{-K_2 a}; \end{aligned}$$

and dividing the two equations

$$K_1 \cot K_1 a = -K_2. \quad (3.13)$$

The effective radius  $a$  of the deuteron can be estimated using the measured binding energy  $\Delta E = 2.22$  Mev and the depth  $V_0 = 33$  MeV (known



from scattering experiments[33]). Solving (3.13) for  $a$  gives  $a \simeq 2.13$  fm. The constants  $B$  and  $D$  are given by the normalization condition  $\int u(r)^* u(r) dr d\Omega = 1$ ; and the normalized wavefunction is

$$u(r) = \begin{cases} 2.21 \sin K_1 r & (r < a) \\ 3.49 \exp(-K_2 r) & (r > a). \end{cases} \quad (3.14)$$

The momentum wavefunction conjugate to  $u(r)/r$  is given by the following Fourier transform (cf. (3.7))

$$\phi(\mathbf{q}_n, \mathbf{q}_p) = \frac{1}{(2\pi)^{3/2}} \int d^3r \frac{u(r)}{r} e^{-i\mathbf{q}\cdot\mathbf{r}} \delta^3(\mathbf{P} - \mathbf{q}_n - \mathbf{q}_p). \quad (3.15)$$

Since  $u(r)$  is spherically symmetric, the z-axis may be chosen for each  $\mathbf{q}$  to lie along  $\mathbf{q}$ . Then the integral can be evaluated:

$$\begin{aligned} \phi(\mathbf{q}_n, \mathbf{q}_p) &= \frac{1}{(2\pi)^{3/2}} \int dr r^2 \sin \theta d\theta d\phi \frac{u(r)}{r} e^{-iqr \cos \theta} \delta^3(\mathbf{P} - \mathbf{q}_n - \mathbf{q}_p) \\ &= \sqrt{\frac{2}{\pi}} \frac{1}{q} \int_0^\infty dr u(r) \sin(qr) \delta^3(\mathbf{P} - \mathbf{q}_n - \mathbf{q}_p) \\ &= \frac{1}{q} \left[ 1.76 \int_0^a dr \sin(K_1 r) \sin(qr) \right. \\ &\quad \left. + 2.78 \int_a^\infty dr e^{-K_2 r} \sin(qr) \right] \delta^3(\mathbf{P} - \mathbf{q}_n - \mathbf{q}_p) \end{aligned}$$

The delta function ensures momentum conservation; and if we take the deuteron to be at rest so that  $\mathbf{P} = 0$ , then the integral is non-zero only when  $\mathbf{q}_n = -\mathbf{q}_p$ . Noting from (3.8) that  $\mathbf{q} = \mathbf{q}_p = -\mathbf{q}_n$  and completing the integration, we have

$$\begin{aligned} \phi(q_n, q_p) &= \phi(q_p) \\ &= \phi(-q_n) \\ &= \frac{1}{q} \left[ 2.78 e^{-K_2 a} \frac{K_2 \sin(qa) + q \cos(qa)}{K_2^2 + q^2} \right. \\ &\quad \left. - 1.76 \frac{K_1 \cos(K_1 a) \sin(qa) - q \sin(K_1 a) \cos(qa)}{K_1^2 - q^2} \right]. \quad (3.16) \end{aligned}$$

A small discovery indeed that the conjugate wavefunction is expressible in closed form! The reader may verify that (3.16) is correctly normalized. The square modulus of this function peaks at  $q = 0$  and drops quickly to zero (see Fig. 3.2).

Figure 3.2:  $|\phi(q)|^2$  vs  $q$

## Inverse Beta Decay

In the first approximation we grant that the cross-section for the reaction

$$\bar{\nu}_e + d \rightarrow n + n + e^+$$

is the same as that for the inverse beta decay

$$\bar{\nu}_e + p \rightarrow n + e^+$$

where the proton has a momentum spectrum given by (3.16). We first consider the process in which the proton is initially at rest (i.e. has fixed momentum). The transition matrix element from 1st-order time-dependent perturbation theory is

$$M = -i \int_{-\infty}^{+\infty} \langle n e^+ | H_{int} | \bar{\nu}_e p \rangle e^{i(E_f - E_i)t} dt$$

When written in terms of a hamiltonian density  $\mathcal{H}_{int}$  that is time-independent, it becomes

$$M = -i \int d^3x \langle n e^+ | \mathcal{H}_{int} | \bar{\nu}_e p \rangle \int_{-\infty}^{+\infty} e^{i(E_f - E_i)t} dt \quad (3.17)$$

In the Cabbibo theory  $\mathcal{H}_{int}$  is written as a product of two fermion current densities  $J_\lambda^\dagger$  and  $j^\lambda$ ;  $M$  then has the decoupled form

$$M = \frac{G}{\sqrt{2}} \cos \theta_C \int d^4x \langle n | J_\lambda^\dagger | p \rangle \langle e^+ | j^\lambda | \bar{\nu}_e \rangle$$

where  $\int d^4x = \int d^3\mathbf{x} dt$ . The current densities have the V-A<sup>1</sup> form[30] given by

$$\begin{aligned} J_\lambda &= \bar{\psi}(V_\lambda - A_\lambda)\psi \\ j^\lambda &= \bar{\psi}\gamma^\lambda(1 - \gamma_5)\psi \end{aligned}$$

where

$$\begin{aligned} V_\lambda(q) &= \gamma_\lambda f_1(q^2) - i \frac{\sigma_{\lambda\nu} q^\nu}{2m} f_2(q^2) + \frac{q_\lambda}{2m} f_3(q^2) \\ A_\lambda(q) &= \left[ \gamma_\lambda g_1(q^2) - i \frac{\sigma_{\lambda\nu} q^\nu}{2m} g_2(q^2) + \frac{q_\lambda}{2m} g_3(q^2) \right] \gamma_5. \end{aligned}$$

---

<sup>1</sup>Vector current minus axial vector current. Note that  $\bar{\psi}\gamma_\mu\gamma_5\psi$  is an axial 4-vector whereas  $\bar{\psi}\gamma^\mu\psi$  is a polar vector, which changes sign under space inversion.



Here the current densities are given as their Fourier conjugates and  $2m = m_p + m_n$ . It can be shown that the form factors  $f_i(q^2), g_i(q^2)$  are dependent only on  $q^2$ . Since only low-energy neutrinos will be dealt with in this calculation, the fact that the nuclear recoil  $\mathbf{p}_n - \mathbf{p}_p = \mathbf{p}_\nu - \mathbf{p}_e = \mathbf{q}$  is small permits the use of the form factors at  $q = 0$ . Henceforth the notation  $f_i = f_i(0)$ ,  $g_i = g_i(0)$  will be used. Note also that 3-vectors are set in boldface whereas 4-vectors are set in lightface and are capitalized.

The conserved vector current (CVC) hypothesis implies that the 4-divergence  $\partial_\lambda \mathcal{V}_\lambda = \partial(\bar{\psi} \mathcal{V}_\lambda \psi)/\partial x^\lambda$ , where  $\mathcal{V}_\lambda(x) = \int V_\lambda(q) e^{iq \cdot x} d^4x$  is the Fourier conjugate of  $V(q)$ , vanishes. This is because the 3-divergence satisfies a continuity equation of the form

$$\frac{\partial(\bar{\psi} \mathcal{V}_i \psi)}{\partial x^i} = \frac{-\partial(\bar{\psi} \mathcal{V}_0 \psi)}{\partial x_0}$$

whence  $\partial(\bar{\psi} \mathcal{V}_\lambda \psi)/\partial x^\lambda = 0$ . Then for a well-behaved  $V(q)$

$$\partial_\lambda \mathcal{V}_\lambda = i \int q_\lambda \bar{\psi} V_\lambda(q) \psi e^{iq \cdot x} d^4x = 0$$

means that  $q_\lambda V_\lambda(q)$  is identically zero. Now consider

$$\begin{aligned} q_\lambda V_\lambda &= q_\lambda \gamma_\lambda f_1(q^2) - i q_\lambda \frac{\sigma_{\lambda\nu} q^\nu}{2m} f_2(q^2) + \frac{q^2}{2m} f_3(q^2) \\ &= 0 \end{aligned}$$

and observe that from the Dirac equation

$$\begin{aligned} \gamma_\lambda q_\lambda \psi &= (\gamma_\lambda p_{p\lambda} - \gamma_\lambda p_{n\lambda}) \psi \\ &= -(m_p - m_n) \psi \\ &\simeq 0 \end{aligned}$$

and that  $q_\lambda \sigma_{\lambda\nu} q^\nu = -q_\nu \sigma_{\nu\lambda} q^\lambda = 0$  since  $\sigma_{\nu\lambda}$  is an antisymmetric tensor; this means we are left with

$$q_\lambda V_\lambda = \frac{q^2}{2m} f_3(q^2) = 0.$$

This requires  $f_3(q^2)$  to be identically zero since in general  $q^2 \neq 0$ . Other arguments using the CVC hypothesis yield  $f_1 = 1$  and  $f_2 \simeq 3.70$ .

The values of  $g_1$  have been determined experimentally to be  $1.26 \pm 0.012$ . But the existence and magnitude of  $g_2(q^2)$  is still unsettled. It is allegedly zero in reference [31] but not so in an experimental result[30] which gives  $g_2 = 4.4 \pm 1.6$ . So the cross-section will be calculated for both values of  $g$  and the answers compared. Some ambiguity also surrounds  $g_3(q^2)$ ; an analysis of experimental data *assuming that*  $g_2(q^2) \equiv 0$  yields

$$g_3(m_\mu^2) = (10 \pm 3) \frac{2m}{m_\mu}$$

where  $m_\mu$  is the muon mass. It will be seen as our work unfolds that  $g_3(q^2)$  contribute negligibly to the matrix element. (In fact it is found that there are no terms to order  $g_3^2$  in the cross-section).

The transition probability  $M^2$  may be obtained by separately evaluating

$$M_j^2 = |\langle e^+ | j^\lambda | \bar{\nu}_e \rangle|^2$$

and

$$M_J^2 = |\langle n | J_\lambda^\dagger | n \rangle|^2.$$

We consider first the squared lepton element

$$\begin{aligned} M_j^2 &= |\langle e^+ | j^\lambda | \bar{\nu}_e \rangle|^2 \\ &= |\langle 0 | d_{\mathbf{p}_e}^{(\bar{s}_e)} \bar{\psi}_{\bar{\nu}_e} \gamma^\lambda (1 - \gamma_5) \psi_e d_{\mathbf{p}_{\bar{\nu}_e}}^{\dagger(\bar{s}_{\bar{\nu}_e})} | 0 \rangle|^2 \end{aligned} \quad (3.18)$$

The fields  $\bar{\psi}_{\bar{\nu}_e}$  and  $\psi_e$  expanded in terms of plane-wave states are

$$\begin{aligned} \bar{\psi}_{\bar{\nu}_e} &= \frac{1}{\sqrt{V}} \sum_{\mathbf{p}_\nu} \sum_{s=1,2} \sqrt{\frac{m_\nu}{E_\nu}} \left[ d_{\mathbf{p}_\nu}^{(s)} \bar{v}^{(s)}(\mathbf{p}_\nu) e^{i\mathbf{p}_\nu \cdot \mathbf{x} - iE_\nu t} + b_{\mathbf{p}_\nu}^{\dagger(s)} \bar{u}^{(s)}(\mathbf{p}_\nu) e^{-i\mathbf{p}_\nu \cdot \mathbf{x} - iE_\nu t} \right] \\ \psi_e &= \frac{1}{\sqrt{V}} \sum_{\mathbf{p}_e} \sum_{s=1,2} \sqrt{\frac{m_e}{E_e}} \left[ b_{\mathbf{p}_e}^{(s)} u^{(s)}(\mathbf{p}_e) e^{i\mathbf{p}_e \cdot \mathbf{x} - iE_e t} + d_{\mathbf{p}_e}^{\dagger(s)} u^{(s)}(\mathbf{p}_e) e^{-i\mathbf{p}_e \cdot \mathbf{x} + iE_e t} \right]. \end{aligned}$$

(See reference [32] for the definitions of the operators  $b_{\mathbf{p}}$ ,  $d_{\mathbf{p}}$  etc). Because of the anticommutation relations for these operators, the  $b_{\mathbf{p}_e}$  operators in the expansion for  $\psi_e$  will commute pass the creation operator for the antineutrino  $d_{\mathbf{p}_{\bar{\nu}_e}}^{\dagger(\bar{s}_{\bar{\nu}_e})}$  in (3.18) to end up at the right edge of the matrix element. Since they are annihilation operators, they act on the vacuum state  $|0\rangle$  to give zero. Similarly all the  $d_{\mathbf{p}_e}^\dagger$  operators in  $\psi_e$  will commute with

both  $\bar{\psi}_{\bar{\nu}_e}$  and  $d_{\mathbf{p}_e}^{(\tilde{s}_e)}$  to end up at the left edge of the matrix element where they act on  $\langle 0|$  to give zero—*except* for the single  $d_{\mathbf{p}_e}^{\dagger(s)}$  whose  $\mathbf{p}_e$  and  $s$  are equal to  $\tilde{\mathbf{p}}_e$  and  $\tilde{s}_e$  associated with  $d_{\tilde{\mathbf{p}}_e}^{(\tilde{s}_e)}$ . Here the anticommutation relation  $\{d_{\mathbf{p}}^{(s)}, d_{\mathbf{p}'}^{\dagger(s')}\} = \delta_{\mathbf{p}\mathbf{p}'}\delta_{ss'}$  implies

$$d_{\mathbf{p}_e}^{(s)} d_{\mathbf{p}_e}^{\dagger(s)} = -d_{\mathbf{p}_e}^{\dagger(s)} d_{\mathbf{p}_e}^{(s)} + 1.$$

The  $d_{\mathbf{p}_e}^{(s)}$  in the first term on the righthand side will not contribute since it acts on  $|0\rangle$ . But the 1 remains and so  $\psi_e$  is effectively replaced by the plane-wave state  $(1/\sqrt{V})\sqrt{m_e/\tilde{E}_e} v_{\tilde{\mathbf{p}}_e}^{(\tilde{s}_e)} e^{-i\tilde{\mathbf{p}}_e \cdot \mathbf{x} + i\tilde{E}_e t}$  where  $\tilde{\mathbf{p}}_e$  and  $\tilde{s}_e$  are the momentum and spin of the positron.

An analogous procedure applied to  $d_{\tilde{\mathbf{p}}_{\bar{\nu}_e}}^{\dagger(\tilde{s}_{\bar{\nu}_e})}$  and the  $b_{\mathbf{p}_\nu}^{\dagger(s)}, d_{\mathbf{p}_\nu}^{(s)}$  operators in the expansion for  $\bar{\psi}_{\bar{\nu}_e}$  replaces the latter in the matrix element with  $\bar{v}_{\tilde{\mathbf{p}}_{\bar{\nu}_e}}^{(\tilde{s}_{\bar{\nu}_e})} e^{-i\tilde{\mathbf{p}}_{\bar{\nu}_e} \cdot \mathbf{x} + i\tilde{E}_{\bar{\nu}_e} t}$ . In general if  $n$  is a particle and  $\bar{n}$  its antiparticle, the rules for such substitutions are the following:

$$\begin{aligned} \psi_n &\rightarrow \frac{1}{\sqrt{V}} \sqrt{\frac{m_n}{E_n}} u^{(s)}(\mathbf{p}_n) e^{i\mathbf{p}_n \cdot \mathbf{x} - iE_n t} \\ \psi_{\bar{n}} &\rightarrow \frac{1}{\sqrt{V}} \sqrt{\frac{m_{\bar{n}}}{E_{\bar{n}}}} v^{(s)}(\mathbf{p}_{\bar{n}}) e^{-i\mathbf{p}_{\bar{n}} \cdot \mathbf{x} + iE_{\bar{n}} t} \\ \bar{\psi}_n &\rightarrow \frac{1}{\sqrt{V}} \sqrt{\frac{m_n}{E_n}} \bar{u}^{(s)}(\mathbf{p}_n) e^{-i\mathbf{p}_n \cdot \mathbf{x} + iE_n t} \\ \bar{\psi}_{\bar{n}} &\rightarrow \frac{1}{\sqrt{V}} \sqrt{\frac{m_{\bar{n}}}{E_{\bar{n}}}} \bar{v}^{(s)}(\mathbf{p}_{\bar{n}}) e^{i\mathbf{p}_{\bar{n}} \cdot \mathbf{x} - iE_{\bar{n}} t} \end{aligned}$$

Thus the squared lepton element becomes

$$M_j^2 = \frac{m_\nu m_e}{E_\nu E_e} \frac{1}{V^2} |\bar{v}^{(s)}(\mathbf{p}_\nu) \gamma^\lambda (1 - \gamma_5) v^{(s)}(\mathbf{p}_e)|^2 \quad (3.19)$$

(the tildes on  $\mathbf{p}$  and  $s$  are dropped). The Lorentz index  $\lambda$  also appears in the squared hadron element  $M_j^2$  and will therefore be contracted when  $M^2$  is evaluated. The part involving spinors in (3.19) can be written as a two-part product

$$|\bar{v}^{(s)}(\mathbf{p}_\nu) \gamma^\lambda (1 - \gamma_5) v^{(s)}(\mathbf{p}_e)|^2$$



$$\begin{aligned}
&= [\bar{v}^{(s)}(\mathbf{p}_\nu)\gamma^\lambda(1-\gamma_5)v^{(s)}(\mathbf{p}_e)] [\bar{v}^{(s)}(\mathbf{p}_\nu)\gamma^\mu(1-\gamma_5)v^{(s)}(\mathbf{p}_e)]^\dagger \\
&= [\bar{v}^{(s)}(\mathbf{p}_\nu)\gamma^\lambda(1-\gamma_5)v^{(s)}(\mathbf{p}_e)] [\{v^{(s)\dagger}(\mathbf{p}_e)\gamma_4\}\gamma_4(1-\gamma_5^\dagger)\gamma^{\mu\dagger}\{\gamma_4v^{(s)}(\mathbf{p}_e)\}] \\
&= [\bar{v}^{(s)}(\mathbf{p}_\nu)\gamma^\lambda(1-\gamma_5)v^{(s)}(\mathbf{p}_e)\bar{v}^{(s)}(\mathbf{p}_e)\gamma^\mu(1-\gamma_5)v^{(s)}(\mathbf{p}_e)] \quad (3.20)
\end{aligned}$$

where we have used the definition of  $\bar{v}^{(s)}$

$$\bar{v}^{(s)} = v^{\dagger(s)}\gamma_4$$

and the fact that for any expression  $\Gamma$  involving  $\gamma$  matrices,

$$\Gamma = \gamma_4\Gamma^\dagger\gamma_4.$$

The index  $\mu$  in (3.20) does not survive since the squared hadron element  $M_J^2$ , when written in a similar two-part form, furnishes an additional index with which it is contracted. Note that this technique is possible because

$$\begin{aligned}
|(M_J)_\lambda(M_J)_\lambda|^2 &= [(M_J)_\lambda(M_J)_\lambda][(M_J)_\mu^\dagger(M_J)_\mu^\dagger] \\
&= [(M_J)_\lambda(M_J)_\mu^\dagger][(M_J)_\lambda(M_J)_\mu^\dagger]
\end{aligned}$$

since  $(M_J)_\lambda$  and  $(M_J)_\lambda$  are *commuting scalars*.

Finally by exposing the matrix indices hidden in the notation of (3.20)

$$[\bar{v}^{(s)}(\mathbf{p}_\nu)]_\alpha[\gamma_\lambda(1-\gamma_5)]_{\alpha\beta}[v^{(s)}(\mathbf{p}_e)\bar{v}^{(s)}(\mathbf{p}_e)]_{\beta\epsilon}[\gamma_\mu(1-\gamma_5)]_{\epsilon\zeta}[v^{(s)}(\mathbf{p}_\nu)]_\zeta$$

we realize when the leftmost term is brought to the right-end that the expression is really the trace of a  $4 \times 4$  matrix. (Note that no matrix index survives). Then the trace theorems in reference [32] can be applied to greatly facilitate the evaluation of  $M_J^2$  and  $M_J^2$ .

Now if the spin states of the antineutrino and positron are not specified, i.e. if the incident antineutrinos are unpolarized and we are indifferent about the spin of the positron (so long as a positron is produced), the spin index  $s$  may be summed over to obtain

$$\begin{aligned}
M_J^2 &= \frac{1}{2} \frac{m_e m_\nu}{E_e E_\nu} \frac{1}{V^2} \\
&\times \text{Trace}\{\gamma_\lambda(1-\gamma_5)[\sum_{s=1,2} v^{(s)}(\mathbf{p}_e)\bar{v}^{(s)}(\mathbf{p}_e)]\gamma_\mu(1-\gamma_5)[\sum_{s=1,2} v^{(s)}(\mathbf{p}_\nu)\bar{v}^{(s)}(\mathbf{p}_\nu)]\}.
\end{aligned}$$

The factor of  $1/2$  comes from averaging over two independent reaction rates, one for  $\bar{\nu}_e(\uparrow) \rightarrow e^+(\uparrow)$  or  $e^+(\downarrow)$  (antineutrino spin-up to positron up or down) and the other for  $\bar{\nu}_e(\downarrow) \rightarrow e^+(\uparrow)$  or  $e^+(\downarrow)$ . Then with the help of the trace theorem (where the *Feynman slash*  $\not{P} \equiv \gamma_\mu P_\mu$ )

$$\sum_s v^{(s)}(\mathbf{p}) \bar{v}^{(s)}(\mathbf{p}) = \frac{-\not{P} + m}{2m}$$

we have

$$\begin{aligned} M_j^2 &= \frac{1}{2} \frac{m_e m_\nu}{E_e E_\nu} \frac{1}{V^2} e^{-i2(\mathbf{p}_e - \mathbf{p}_\nu) \cdot \mathbf{x}} \\ &\times \text{Trace} \left\{ \gamma_\lambda (1 - \gamma_5) \left( \frac{-\not{P}_e + m_e}{2m_e} \right) \gamma_\mu (1 - \gamma_5) \left( \frac{-\not{P}_\nu + m_\nu}{2m_\nu} \right) \right\}. \end{aligned}$$

The above expression can now be expanded and simplified using various other trace theorems (see [32]) to obtain

$$\begin{aligned} M_j^2 &= \frac{1}{2} \frac{m_e m_\nu}{E_e E_\nu} \frac{1}{V^2} \\ &\times \left[ \frac{2}{m_e m_\nu} (P_{e\lambda} P_{\nu\mu} - \delta_{\lambda\mu} P_e \cdot P_\nu + P_{e\mu} P_{\nu\lambda} + i\epsilon_{\lambda\mu\sigma\rho} P_{e\sigma} P_{\nu\rho}) \right] \\ &= \frac{e^{-i2(\mathbf{p}_e - \mathbf{p}_\nu) \cdot \mathbf{x}}}{E_e E_\nu V^2} (P_{e\lambda} P_{\nu\mu} - \delta_{\lambda\mu} P_e \cdot P_\nu + P_{e\mu} P_{\nu\lambda} + i\epsilon_{\lambda\mu\sigma\rho} P_{e\sigma} P_{\nu\rho}) \end{aligned} \quad (3.21)$$

The squared hadron element begins as

$$\begin{aligned} M_J^2 &= \frac{m_n m_p}{E_n E_p} \frac{1}{V^2} \\ &\times \left| \bar{u}^{(s)}(\mathbf{p}_n) \left[ \gamma_\lambda (f_1 - g_1 \gamma_5) - i \frac{\sigma_{\lambda\nu} q^\nu}{2m} (f_2 - g_2 \gamma_5) - \frac{q_\lambda}{2m} (f_1 - g_3 \gamma_5) \right] u^{(s)}(\mathbf{p}_p) \right|^2 \end{aligned}$$

When written as a trace with the sum over initial and final spin states implemented, it becomes

$$\begin{aligned} M_J^2 &= \frac{1}{2} \frac{m^2}{E_n E_p} \frac{1}{V^2} e^{-i2(\mathbf{p}_p - \mathbf{p}_n) \cdot \mathbf{x}} \\ &\times \text{Trace} \left\{ \left[ \gamma_\lambda (f_1 - g_1 \gamma_5) - i \frac{\sigma_{\lambda\nu} q^\nu}{2m} (f_2 - g_2 \gamma_5) - \frac{q_\lambda}{2m} (f_1 - g_3 \gamma_5) \right] \left( \frac{\not{P}_p + m}{2m} \right) \right. \\ &\times \left. \left[ \gamma_\mu (f_1 - g_1 \gamma_5) - i \frac{\sigma_{\mu\nu} q^\nu}{2m} (f_2 - g_2 \gamma_5) - \frac{q_\mu}{2m} (f_1 - g_3 \gamma_5) \right] \left( \frac{\not{P}_n + m}{2m} \right) \right\} \end{aligned}$$

where  $m = (m_n + m_p)/2$  has been written for both  $m_n$  and  $m_p$  and the trace theorem

$$\sum_s u^{(s)}(\mathbf{p}) \bar{u}^{(s)}(\mathbf{p}) = \frac{\not{p} + m}{2m}$$

has been used. Considering only the term in  $g_3$ , it is found that

$$g_3^2 \text{Trace} \left\{ \frac{q_\lambda}{2m} \gamma_5 \left( \frac{\not{p}_n + m}{2m} \right) \frac{q_\lambda}{2M} \gamma_5 \left( \frac{\not{p}_p + m}{2m} \right) \right\}$$

when contracted with

$$(P_{e\lambda} P_{\nu\mu} - \delta_{\lambda\mu} P_e \cdot P_\nu + P_{e\mu} P_{\nu\lambda} + i\epsilon_{\lambda\mu\sigma\rho} P_{e\sigma} P_{\nu\rho})$$

from (3.21) gives a zero result. This means that there are no terms of order  $g_3^2$  in the squared matrix element. Since in fact there is reason to think that  $g_3(q^2)$  at  $q \simeq 0$  is small, it will be neglected in our calculation. The details of the trace calculation are messy and will be omitted.

The answer, when all indices are contracted, is

$$\begin{aligned} M_J^2 M_J^2 &= \frac{-1}{4V^4 E_n E_p E_\nu E_e} \left[ 2P_p \cdot P_e P_e \cdot P_\nu P_e \cdot P_n m^{-2} (f_2^2 - g_2^2) \right. \\ &\quad - 4P_p \cdot P_e P_e \cdot P_\nu (f_1 g_1 + g_1 g_2) - 2P_p \cdot P_e P_e \cdot P_n (f_1^2 + 2f_1 g_1 + g_1^2) \\ &\quad + 2P_p \cdot P_e m_\nu^2 (f_1 g_1 + g_1 g_2) + P_p \cdot P_\nu P_e \cdot P_\nu P_\nu \cdot P_n m^{-2} (f_2^2 - g_2^2) \\ &\quad + 4P_p \cdot P_\nu P_e \cdot P_\nu (g_1 g_2 - f_1 g_2) + 4P_p \cdot P_\nu P_e \cdot P_n (2f_1 g_1 - f_1^2 - g_1^2) \\ &\quad - 2P_p \cdot P_\nu P_\nu \cdot P_n m^{-2} m_e^2 (f_2^2 - g_2^2) + 2P_p \cdot P_\nu m_e^2 (2f_1 g_2 - g_1 g_2) \\ &\quad - 1/2 P_p \cdot P_n P_e \cdot P_\nu m^{-2} m_e^2 (f_2^2 - g_2^2) - 1/2 P_p \cdot P_n P_e \cdot P_\nu m^{-2} m_\nu^2 (f_2^2 - g_2^2) \\ &\quad + P_p \cdot P_n m^{-2} m_e^2 m_\nu^2 (f_2^2 - g_2^2) + 2(P_e \cdot P_\nu)^2 (f_2^2 + g_2^2) \\ &\quad + 4P_e \cdot P_\nu P_e \cdot P_n (f_1 g_1 - g_1 g_2) + 4P_e \cdot P_\nu P_\nu \cdot P_n (f_1 g_1 + g_1 g_2) \\ &\quad + 4P_e \cdot P_\nu m^2 (f_1^2 - g_1^2) - 3/2 P_e \cdot P_\nu m_e^2 (f_1^2 + g_1^2) \\ &\quad - 3/2 P_e \cdot P_\nu m_\nu^2 (f_1^2 + g_1^2) - 2P_e \cdot P_n m_\nu^2 (2f_1 g_2 - g_1 g_2) \\ &\quad \left. - 2P_\nu \cdot P_n m_e^2 (2f_1 g_2 + g_1 g_2) + m_e^2 m_\nu^2 (f_2^2 + g_2^2) \right] \end{aligned}$$

For the case in which  $g_3 = g_2 = 0$  while the other form factors have values as given earlier, we have the result

$$M_J^2 M_J^2 = \frac{1}{4V^4 E_n E_p E_\nu E_e} \left[ 3.1053 \times 10^{-5} P_p \cdot P_e P_e \cdot P_\nu P_e \cdot P_n \right.$$



$$\begin{aligned}
& + 20.43 P_p \cdot P_e P_\nu \cdot P_n - 3.1053 \times 10^{-5} P_p \cdot P_\nu P_e \cdot P_\nu P_\nu \cdot P_n \\
& + 0.2704 P_p \cdot P_\nu P_e \cdot P_n + 8.1086 \times 10^{-6} P_p \cdot P_\nu P_\nu \cdot P_n \\
& + 2.0271 \times 10^{-6} P_p \cdot P_n P_e \cdot P_\nu - 27.38 (P_e \cdot P_\nu)^2 \\
& + 2.072 \times 10^6 P_e \cdot P_\nu ]
\end{aligned}$$

Here numerical values have also been substituted for  $m, m_e$  and  $m_\nu (= 0)$ . The case in which  $g_2 = 4.4, g_3 = 0$  is also given below for completeness:

$$\begin{aligned}
M_J^2 M_J^2 &= \frac{1}{4V^4 E_n E_p E_\nu E_e} \left[ 1.286 \times 10^{-5} P_p \cdot P_e P_e \cdot P_\nu P_e \cdot P_n \right. \\
& + 39.78 P_p \cdot P_e P_e \cdot P_\nu + 20.43 P_p \cdot P_e P_\nu \cdot P_n \\
& + 1.286 \times 10^{-5} P_p \cdot P_\nu P_e \cdot P_\nu P_\nu \cdot P_n - 4.576 P_p \cdot P_\nu P_e \cdot P_\nu \\
& + 0.2704 P_p \cdot P_\nu P_e \cdot P_n - 3.358 \times 10^{-6} P_p \cdot P_\nu P_\nu \cdot P_n \\
& - 1.700 P_p \cdot P_\nu - 8.396 \times 10^{-7} P_p \cdot P_n P_e \cdot P_\nu \\
& - 66.10 (P_e \cdot P_\nu)^2 + 4.576 P_e \cdot P_\nu P_e \cdot P_n \\
& \left. - 39.78 P_e \cdot P_\nu P_\nu \cdot P_n + 2.072 \times 10^6 P_e \cdot P_\nu + 7.491 P_\nu \cdot P_n \right]
\end{aligned}$$

If only low energy neutrinos are considered (such as those from the Sun whose energies are typically  $\leq 15\text{MeV}$ ), the highlighted term in the above expression overwhelms the rest by a factor of about 100. The same dominant term also occurs in the result where  $g_2$  has the value zero instead of 4.4. Then to within a few percent of the final cross-section result—regardless of the choice of  $g_2$ —we may approximate  $M^2$  by

$$\begin{aligned}
M^2 &\simeq \left( \frac{G^2}{2} \cos^2 \theta_C \right) \frac{1}{4V^4} \frac{20.43}{E_n E_p E_\nu E_e} (P_p \cdot P_e P_\nu \cdot P_n) \\
&\times \left[ \int d^4x \ e^{i(P_n + P_e - P_p - P_\nu)t} \right]^2.
\end{aligned}$$

From a textbook<sup>2</sup> calculation using a  $\sin x/x$  representation of the  $\delta$ -function, we have

$$\begin{aligned}
\left[ \lim_{T \rightarrow \infty} \int_{-T/2}^{T/2} d^4x \ e^{i(P_n + P_e - P_p - P_\nu) \cdot x} \right]^2 &= 2\pi T \delta(E_n + E_e - E_p - E_\nu) \\
&\times (2\pi)^3 V \delta^3(\mathbf{p}_n + \mathbf{p}_e - \mathbf{p}_p - \mathbf{p}_\nu)
\end{aligned}$$

---

<sup>2</sup>See for example Harris in [32]

So the transition probability rate is

$$\frac{M^2}{T} \simeq \left( \frac{G^2}{2} \cos^2 \theta_C \right) \frac{(2\pi)^4}{V^3} \frac{5.108}{E_n E_p E_\nu E_e} (P_p \cdot P_e P_\nu \cdot P_n) \delta^4(P_n + P_e - P_p - P_\nu). \quad (3.22)$$

## Averaged Cross-Section

Since the transition rate is sought for a proton with a distributed momentum, the result in (3.22) must be averaged over the momentum spectrum given by (3.16). The average, when the momenta of the final-state particles are summed over, is

$$N = \int_{\mathbf{p}_p} d^3 \mathbf{p}_p \sum_{\mathbf{p}_n} \sum_{\mathbf{p}_e} \frac{M^2}{T} |\phi(p_p)|^2 \quad (3.23)$$

In the continuum limit as  $V \rightarrow \infty$ ,  $(1/V) \sum_{\mathbf{p}}$  is replaced by  $1/(2\pi)^3 \int_{\mathbf{p}} d^3 \mathbf{p}$  and so we have

$$\begin{aligned} N &= \frac{1}{(2\pi)^2 V} \int_{\mathbf{p}_p} \int_{\mathbf{p}_n} \int_{\mathbf{p}_e} d^3 \mathbf{p}_p d^3 \mathbf{p}_n d^3 \mathbf{p}_e \\ &\times \frac{5.108}{E_n E_p E_\nu E_e} (P_p \cdot P_e P_\nu \cdot P_n) |\phi(p_p)|^2 \delta^4(P_n + P_e - P_p - P_\nu) \end{aligned} \quad (3.24)$$

Since the  $\delta$ -function of 4-momenta, the inner products and the combination  $\frac{d^3 \mathbf{p}}{E}$  are all Lorentz invariant, we will profit by evaluating the manifestly Lorentz invariant expression

$$N' = \int_{\mathbf{p}_n} \int_{\mathbf{p}_e} \frac{d^3 \mathbf{p}_n}{E_n} \frac{d^3 \mathbf{p}_e}{E_e} (P_p \cdot P_e P_\nu \cdot P_n) \delta^4(P_n + P_e - P_p - P_\nu)$$

in a frame in which the proton is at rest and the antineutrino is incident in the z-direction. The  $\delta$ -function replaces every  $\mathbf{p}_e$  (say) with  $\mathbf{p}_\nu + \mathbf{p}_p - \mathbf{p}_n$  and relieves us of the  $d^3 \mathbf{p}_e$  integration. Noting that  $p_e^2 = (\mathbf{p}_\nu - \mathbf{p}_n)^2 = \sqrt{p_\nu^2 + p_n^2 - 2p_n p_\nu \cos \theta_n + m_e^2}$  there is then

$$\begin{aligned} N' &= \int p_n^2 \sin \theta_n d\theta_n d\phi_n dp_n \frac{(P_p \cdot P_e P_\nu \cdot P_n)}{E_n E_e} \\ &\times \delta(\sqrt{p_n^2 + m^2} + \sqrt{p_\nu^2 + p_n^2 - 2p_n p_\nu \cos \theta_n + m_e^2} - m - p_\nu) \end{aligned} \quad (3.25)$$

where  $\phi_n$  and  $\theta_n$  are the polar and azimuthal angles for the neutron. The  $\phi_n$  integration is trivial since we have azimuthal symmetry. The theorem

$$\delta(f(z)) = \sum_{z_0} \frac{z - z_0}{|\partial f / \partial z|_{z_0}}$$

where  $z_0$ 's are zeros of  $f(z)$  can be usefully applied here if we take  $z$  to be  $\cos \theta_n$  (with  $dz = -\sin \theta_n d\theta_n$ ) and  $f(z) = \sqrt{p_n^2 + m^2} + \sqrt{p_\nu^2 + p_n^2 - 2p_n p_\nu z + m_e^2}$ . Then the  $\delta$ -function in (3.25) simplifies to

$$\begin{aligned} & \frac{\delta(z_n - z_{n_0})}{p_\nu p_n / \sqrt{p_\nu^2 + p_n^2 - 2p_n p_\nu z_0 + m_e^2}} \\ &= \frac{\delta(z - z_0)}{p_\nu p_n} [p_\nu + m - \sqrt{p_n^2 + m^2}] \end{aligned}$$

since  $z_0$  satisfies  $p_\nu + m - \sqrt{p_n^2 + m^2} = \sqrt{p_\nu^2 + p_n^2 - 2p_n p_\nu z_0 + m_e^2}$ . If we replace  $p_n dp_n$  with  $E_n dE_n$  and note that  $p_\nu + m - \sqrt{p_n^2 + m^2}$  is just  $E_e$ , then

$$\begin{aligned} N' &= 2\pi \int dE_n \frac{(P_p \cdot P_e P_\nu \cdot P_n)}{p_\nu} \\ &= 2\pi \int dE_n \frac{m E_e}{p_\nu} (P_\nu E_n - P_\nu P_n z_0). \end{aligned}$$

And when

$$z_0 = \frac{(p_\nu + m)\sqrt{p_n^2 + m^2} - p_\nu m - m^2 + m_e^2/2}{p_\nu p_n}$$

is substituted, the integral can be evaluated analytically to obtain

$$N' = \frac{m^2}{p_\nu} \left[ \frac{(p_\nu + m - E_n)^2}{4m} m_e^2 - \frac{(p_\nu + m - E_n)^3}{3} \right]_{E_{n_{\min}}}^{E_{n_{\max}}} \quad (3.26)$$

where  $E_{n_{\max}}, E_{n_{\min}}$  are the kinematic limits on the neutron energy. The transition rate can be cast into a manifestly Lorentz invariant form using the identification  $|\mathbf{p}_\nu| = (P_\nu \cdot P_p)/m$  and  $E_n = (P_n \cdot P_p)/m$ :

$$\begin{aligned} N &= \int p_p^2 dp_p d\phi_p dz \frac{5.108 |\phi(p_p)|^2}{2\pi V E_p p_\nu} \left\{ \frac{m^3}{P_\nu \cdot P_p} \left[ \frac{(P_\nu \cdot P_p/m + m - P_n \cdot P_p/m)^2}{4m} m_e^2 \right. \right. \\ &\quad \left. \left. - \frac{(P_\nu \cdot P_p/m + m - P_n \cdot P_p/m)^3}{3} \right]_{E_{n_{\min}}}^{E_{n_{\max}}} \right\} \quad (3.27) \end{aligned}$$



The total cross-section is related to the transition probability rate  $N$  (cf. (3.3)) by

$$\int \sigma d\Omega = \frac{N}{J_{inc}}$$

with the incident flux given by

$$J_{inc} = \frac{c}{V}$$

where  $c = 1$  is the velocity of the antineutrino and  $1/V$  the number density. The expression for the cross-section per incident antineutrino is then

$$\begin{aligned} \sigma_{tot} = & \int p_p^2 dp_p dz \frac{5.108 |\phi(p_p)|^2}{E_p p_\nu} \left\{ \frac{m^3}{P_\nu \cdot P_p} \left[ \frac{(P_\nu \cdot P_p/m + m - P_n \cdot P_p/m)^2}{4m} m_e^2 \right. \right. \\ & \left. \left. - \frac{(P_\nu \cdot P_p/m + m - P_n \cdot P_p/m)^3}{3} \right]_{E_{nmax}}^{E_{nmin}} \right\} \end{aligned} \quad (3.28)$$

where we have effected the trivial integration over  $\phi_p$ .

## Kinematic Limits

The limits  $E_{nmax}, E_{nmin}$  are convergent at the threshold and will in general diverge as the energy available for the reaction increases. In (3.27) it is seen that  $N$  vanishes when  $E_{nmax} = E_{nmin}$ . The existence of a threshold at which the cross-section vanishes is a purely kinematic effect, since the matrix element does not vanish even for processes that are ‘off the mass shell’ (i.e. for which the particles involved do not satisfy  $E^2 \neq p^2 + m^2$ ). Therefore to obtain a correct threshold effect,  $E_{nmax}$  and  $E_{nmin}$  must be the kinematic limits for the reaction  $\bar{\nu}_e d \rightarrow n n e^+$ . But because the field theory calculation is of the  $\bar{\nu}_e p \rightarrow n e^+$  reaction rate, the  $\delta$ -function in (3.25) obliges us to substitute  $\mathbf{p}_\nu + \mathbf{p}_p - \mathbf{p}_n$  for  $\mathbf{p}_e$ , thereby apparently conserving momentum for the reaction  $\bar{\nu}_e p \rightarrow n e^+$  (and thereby infracting momentum conservation for  $\bar{\nu}_e d \rightarrow n n e^+$ ). Hence one wonders whether momentum conservation is calculationally violated. Nevertheless it may be argued that once the  $\bar{\nu}_e p \rightarrow n e^+$  reaction rate is obtained and convolved with the  $p_p$  spectrum, the total available momentum for the reaction  $\bar{\nu}_e d \rightarrow n n e^+$  will be carried by the antineutrino—we can assume without loss of ground that the deuteron is at rest—since the momentum of the bound proton

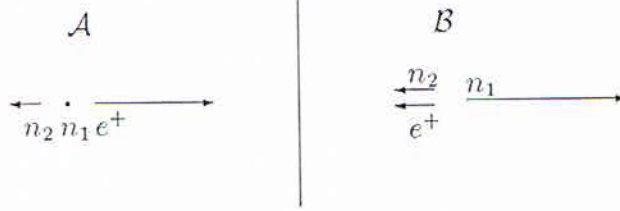


Figure 3.3: Kinematic configurations for minimum ( $\mathcal{A}$ ) and maximum ( $\mathcal{B}$ ) neutron energy in the CM frame of the antineutrino and deuteron.

is canceled by that of the bound neutron. Then even though the proton may have a large momentum, the momentum transferred to the final-state particles must come only from the antineutrino.

The kinematic configurations for maximum and minimum neutron energy are shown in Figure 3.3. Configuration  $\mathcal{A}$  is permitted for all  $E_\nu > E_{\nu_{th}} + 0.01$  MeV where  $E_{\nu_{th}}$  is the threshold energy (4.03 MeV) for the reaction. To prove this, we will first confirm our suspicion that the configuration is allowed kinematically. The energy and momentum conservation equations are

$$\begin{aligned} E_\nu + m_d &= E_n + E_e + m_n \\ p_\nu^2 &= (\mathbf{p}_n + \mathbf{p}_e)^2 \end{aligned} \quad (3.29)$$

The positive-semi-definiteness of the 4-momenta inner product

$$E_1 \cdot E_2 - \mathbf{p}_1 \cdot \mathbf{p}_2 \geq 0$$

leads to the observation that

$$(E_n + E_e)^2 - (\mathbf{p}_n + \mathbf{p}_e)^2 \geq (m_n + m_e)^2. \quad (3.30)$$

Upon substituting  $E_\nu + m_d - m_n$  for  $E_n + E_e$  from (3.29) and solving for  $E_\nu$ , (3.30) becomes

$$E_\nu \geq \frac{(m_n + m_e)^2 - (m_d - m_n)^2}{2(m_d - m_n)}$$

Comparing this with the threshold kinetic energy  $E_{\nu_{th}}$  given by the standard formula

$$\begin{aligned} E_{\nu_{th}} &= \frac{(M_f - M_i)(M_f + M_i)}{2m_t} \\ &= \frac{(2m_n + m_e - m_d)(2m_n + m_e + m_d)}{2m_d} \end{aligned}$$

where  $M_f, M_i$  are the total final and initial masses and  $m_t$  the mass of the target particle, we realize that

$$E_\nu \geq E_{\nu_{th}} + 0.01 \text{ MeV.}$$

This means that configuration  $\mathcal{A}$  is *not* allowed for the range of energies from  $E_{\nu_{th}}$  to  $E_{\nu_{th}} + 0.01 \text{ MeV}$ . But for the small range one might as well say that  $E_\nu > E_{\nu_{th}}$  and that  $\mathcal{A}$  is allowed for all energies above threshold.

It is indicated in configuration  $\mathcal{B}$  that the neutron  $n_1$  attains its maximum energy when the other neutron  $n_2$  and the positron go off in the opposite direction *with the same velocity*. To see this, consider the three particles in the CM frame of the deuteron and  $\bar{\nu}_e$ . Clearly no momentum will be ‘wasted’ if the directions of  $n_2$  and  $\bar{\nu}_e$  are opposite to that of  $n_1$ . If further  $n_2$  and  $\bar{\nu}_e$  were to have the same velocity, then a frame can be found in which both are at rest, hence have minimum energy, whereupon  $n_1$  must have the maximum energy possible. It can be shown that the configuration that gives a particle the maximum energy in the CM frame will give it the maximum energy possible in any other frame.

Now the total energy available for the reaction in the CM frame is

$$\begin{aligned} E_{CM}^2 &= (p_\nu + m_d)^2 - p_\nu^2 \\ &= 2p_\nu m_d + m_d^2. \end{aligned}$$

The equal-velocities condition

$$\frac{p_{n_2}}{E_{n_2}} = \frac{p_e}{E_e}$$

will be more useful when written as

$$\frac{p_{n_2}}{m_n} = \frac{p_e}{m_e}.$$



Then energy and momentum conservation gives

$$\begin{aligned}
p_{n_1} &= p_{n_2} + p_e = p_{n_2} \left(1 + \frac{m_e}{m_n}\right) \\
E_{n_1} &= E_{CM} - E_{n_2} - E_e \\
&= E_{CM} - \sqrt{p_{n_2}^2 + m_n^2} - \sqrt{p_e^2 + m_e^2} \\
&= E_{CM} - \left(1 + \frac{m_e}{m_n}\right) E_{n_2}.
\end{aligned}$$

The steps that lead to  $E_{n_1}$  in terms of  $p_\nu$  and the masses are as follows:

$$\begin{aligned}
\left(\frac{E_{CM} - E_{n_1}}{1 + m_e/m_n}\right)^2 &= E_{n_2}^2 = (p_{n_2}^2 + m_n^2) \\
&= \left[\left(\frac{p_{n_1}}{m_n + m_e}\right)^2 + 1\right] m_n^2
\end{aligned}$$

So

$$\begin{aligned}
E_{CM}^2 + E_{n_1}^2 - 2E_{CM}E_{n_1} &= p_{n_1}^2 + (m_n + m_e)^2 \\
E_{CM}^2 - 2E_{CM}E_{n_1} &= m_e^2 + 2m_n m_e
\end{aligned}$$

and

$$\begin{aligned}
E_{n_1} &= \frac{E_{CM}^2 - m_e^2 - 2m_n m_e}{2E_{CM}} \\
&= \frac{2p_\nu m_d + m_d^2 - m_e^2 - 2m_n m_e}{4p_\nu m_d + 2m_d^2}
\end{aligned}$$

Transforming back to the rest frame of the deuteron gives

$$E_{n_{max}} = \frac{1}{\sqrt{1 - \beta^2}}(E_{n_1} + \beta p_{n_1})$$

where

$$\beta = \frac{P_\nu}{P_\nu + m_d}.$$

Configuration  $\mathcal{B}$  is permitted for all  $E_\nu$  above threshold. The graphs of  $E_{n_{max}}$  and  $E_{n_{min}}$  are plotted in Figure 3.4;  $E_{n_{min}}$  is horizontal at  $m_n = 939.6$

Figure 3.4: Phase space limits on the neutron energy for  $\bar{\nu}_e d \rightarrow n n e^+$

MeV except for the very small region right above threshold shown in the inset. The permitted neutron energies lie within the wedge shape area.

The Lorentz invariant expression within curly brackets in (3.28) can be evaluated in any frame. For our choice the rest frame of the deuteron, we have

$$\frac{P_n \cdot P_p}{m} = \frac{E_n E_p - p_n p_p \cos \theta_p}{m}$$

since the neutron is either at rest (minimum energy), in which case  $p_n = 0$  and the cosine term does not matter, or moving with maximum energy, in which case it must travel along the incident direction of the antineutrino (z-axis). The integral over  $\theta_p$  and  $p_p$  in (3.28) was evaluated numerically and the answer plotted in Figure 3.5.

Distressingly a comparison of the our total cross-section result with those of Ying et al[29] shows not even an order-of-magnitude agreement (see column (1) in Table 3.1). In fact the graph does not even appear like that of a properly calculated cross-section. However, if the kinematic limits on the neutron energy for the reaction  $\bar{\nu}_e p \rightarrow n e^+$  were used instead, there is *fair* agreement (see column (2)) for incident energies above  $\sim 10$  MeV (i.e. those far above the threshold of the deuterium reaction). Since these limits converge as they should at the lower limit of  $\sim 0.5$  MeV, which is the threshold for  $\bar{\nu}_e p \rightarrow n e^+$ , any agreement with Ying's results is obviously impossible for low energies. The cross-section calculated using these limits is plotted in Figure 3.7.

Table 3.1: Comparison of cross-section results.

$E_\nu$ (MeV)	$\sigma_{tot}$ ( $10^{-42}\text{cm}^2$ )		
	KJ-MLT (1)	KJ-MLT (2)	Ying
5	$1.58 \times 10^1$	$6.48 \times 10^{-1}$	$2.48 \times 10^{-2}$
10	$4.70 \times 10^1$	$3.73 \times 10^0$	$1.23 \times 10^0$
20	$6.39 \times 10^1$	$1.69 \times 10^1$	$1.12 \times 10^1$
30	$1.01 \times 10^2$	$3.84 \times 10^1$	$3.55 \times 10^1$

To discover the kinematic configurations in which the neutron in the process  $\bar{\nu}_e p \rightarrow n e^+$  has limiting energies, consider the CM frame of the proton and antineutrino. There the neutron and positron will go back-to-back



Figure 3.5: Deuterium-neutrino total cross-section calculated using  $\bar{\nu}_e d \rightarrow nne^+$  phase space limits.

along any direction. Hence the directions that give the neutron maximum and minimum energies are respectively those parallel and antiparallel to that of the boost to the CM frame (i.e. along the direction of the incident antineutrino). The limits  $E_{nmax,min} = E_{+,-}$  are

$$\begin{aligned}
E_{+,-} &= \frac{1}{2(m_p^2 + 2m_p p_\nu)} \left\{ (p_\nu + m_p)(p_\nu^2 + 2m_p p_\nu + m_n^2 + m_p^2 - m_e^2) \right. \\
&\quad \pm \left[ (p_\nu + m_p)^2 (p_\nu^2 + 2m_p p_\nu + m_n^2 + m_p^2 - m_e^2)^2 \right. \\
&\quad \left. \left. - (m_p^2 + 2m_p p_\nu)(p_\nu^2 + 2m_p p_\nu + m_n^2 + m_p^2 - m_e^2 + 4p_\nu^2 m_p^2) \right]^{(1/2)} \right\}
\end{aligned} \tag{3.31}$$

which the reader may derive from

$$\begin{aligned}
p_e &= p_n \pm p_\nu \\
E_\nu + m_p &= E_e + E_n
\end{aligned}$$

(and indeed simplify!) This expression yields the correct threshold as the phase space plot in Figure 3.6 shows.

The matrix element as a function of the 4-momenta of the interacting particles is expected to be fairly uniform over the small range of incident energies that are being considered. So the cross-section can depend substantially only on the phase space limits of the reaction. (One can perforce think of the cross-section as  $\int_{E_-}^{E_+} M^2 \delta(\mathbf{p}_i) d^3 \mathbf{p}_i / E_i \sim M^2 \int_{E_-}^{E_+} \delta(\mathbf{p}_i) d^3 \mathbf{p}_i / E_i$  (cf. (3.23)). An inspection of the phase space spectra (Figures 3.4 and 3.7) for the inverse beta and deuterium reactions reveals that although the lower boundary for both are approximately equal, the upper boundary for the latter reaction rises about twice as fast. From this arose the difference between the two results in column (1) and (2) of Table 3.1, since the cross-section increases roughly as  $(E_+ - E_-)^3$ . Now which result is the more meaningful? One can say that the result in column (2) is valid only for energies above  $\sim 10$  Mev (and it should really drop to zero at the threshold of  $\sim 4$  MeV for the deuterium reaction). The problem for the result in column (1) is that we have imposed a set of kinematic limits from one process on a matrix element for a different process. The argument given earlier for this imposition have perhaps come to no avail.

Figure 3.6: Phase space limits on the neutron energy for  $\bar{\nu}_e p \rightarrow n e^+$ .



Figure 3.7: Neutrino-deuterium cross-section calculated using  $\bar{\nu}_e p \rightarrow n e^+$  phase space limits.

## Better Approximation

The preceding analysis takes no account of the Pauli exclusion of the final-state neutrons. To do so one has to obtain their wavefunctions, as follows. Since the spectator neutron retains its momentum distribution from the bound state, its wavefunction is

$$\psi_2(p_2, s_2) = \phi(p_2)\sigma(s_2)$$

where  $\sigma$  is a spin-wavefunction. The other neutron comes from the proton and has the wavefunction

$$\psi_1(p_1, s_1) = M(P_1, P_p, P_\nu, P_e, s_1, s_p)\phi(p_p)\sigma(s_p) \quad (3.32)$$

where  $M$  is the transition matrix element in (3.17). To give (3.32) the character of an average over the ‘input’ proton states,  $p_p$  should really be integrated over. But this will be deferred until the antisymmetrized wavefunction is ready to be squared. It is not necessary to integrate over the spin states  $s_p$  if we assume the proton is unlikely to flip its spin so that  $s_1$  can be identified with  $s_p$ .

The joint wavefunction of the neutrons is then

$$\begin{aligned} \psi(p_1, s_1; p_2, s_2) &= \frac{1}{\sqrt{2}}[\psi_1(p_1, s_1)\psi_2(p_2, s_2) - \psi_1(p_2, s_2)\psi_2(p_1, s_1)] \\ &= \frac{1}{\sqrt{2}}[M(P_1, P_p, s_1, s_p, \dots)\phi(p_p)\phi(p_2)\sigma(s_1)\sigma(s_2) \\ &\quad - M(P_2, P_p, s_2, s_p, \dots)\phi(p_p)\phi(p_1)\sigma(s_2)\sigma(s_1)] \\ &= \frac{1}{\sqrt{2}}[M(P_1, P_p, s_1, s_p, \dots)\phi(p_p)\phi(p_2) \\ &\quad - M(P_2, P_p, s_2, s_p, \dots)\phi(p_p)\phi(p_1)]\sigma(s_1)\sigma(s_2) \end{aligned}$$

The total cross-section is related to the probability  $N_A$  of getting two properly Pauli-excluded neutrons by

$$\sigma_{tot} = \frac{N_A}{J_{inc}}$$

where

$$N_A = \int d^3\mathbf{p}_e d^3\mathbf{p}_1 d^3\mathbf{p}_2 d^3\mathbf{p}_p \left| \sum_{s_1, s_2} \psi(p_1, s_1; p_2, s_2) \right|^2.$$

Since a very large number of terms will arise when  $|\sum \psi|^2$  is evaluated, our calculation will adjourn here. To the student who wishes to complete this problem, we will point to a possible simplification in that no spin-wavefunctions will appear in the final result for  $|\sum \psi|^2$ . This is because  $\sigma(s_1)\sigma(s_2)$  can be expanded in the spin basis states

$$\sigma(1/2)\sigma(1/2), \sigma(1/2)\sigma(-1/2), \sigma(-1/2)\sigma(1/2), \sigma(-1/2)\sigma(-1/2)$$

(or in fact also in the symmetric triplet spin states since the nucleons have parallel spins); and so by virtue of their orthonormality, only spatial terms remain when  $\psi$  is squared with the spin sums implemented.

### 3.3 Conclusion

#### Critique

The cross-section for the reaction  $\bar{\nu}_e d \rightarrow nne^+$  was calculated using a spectator-neutron model for the interaction without accounting for the Pauli exclusion of the final-state neutrons. The interaction is represented as one between only the  $\bar{\nu}_e$  and the bound proton having a distributed momentum that is specified by the deuteron ground state. This representation and the calculation on which it is based are unsatisfactory because:

1. The picture of a  $\bar{\nu}_e$  engaging selectively the proton and turning it into a neutron while leaving the other neutron intact is unrealistic. Moreover the structure of the deuteron has to be investigated since it is necessary to know how the proton is being ‘presented’ to the  $\bar{\nu}_e$ . This introduces the bound state description which is relativistically inadmissible (see item 2). One could either avoid the structure and bound state issue by depicting the interaction as between a  $\bar{\nu}_e$  and the deuteron treated as an elementary particle or use a nonrelativistic theory for the calculation. The former alternative may perhaps be pursued in another project, although the form factors for the corresponding process (see [26]) are complicated and rather inaccessible to the student at this stage.
2. Relativistically the deuteron mass is associated with an energy which fixes the momenta of the proton and neutron (which are equal and



opposite by momentum conservation). But the momenta cannot be fixed—or else the particles will be free—in a bound state. Therefore either energy cannot be conserved in a bound state or such a state cannot exist. More fundamentally the potential well is really instantaneous action-at-a-distance which is not permitted in a relativistic theory. A consistent relativistic treatment of the bound state still awaits discovery.

3. A consequence of at once applying both relativistic quantum field theory and a bound state description is the dilemma of two incompatible 4-momentum (i.e. energy and momentum) conservation requirements. One is built into the field theory that was used to calculate the transition rate for the process  $\bar{\nu}_e p \rightarrow n e^+$ . It manifests as the  $\delta$ -function in (3.8) and conserves 4-momentum for the process  $\bar{\nu}_e p \rightarrow n e^+$ . The other requirement conserves 4-momentum for the process  $\bar{\nu}_e d \rightarrow n n e^+$  and was imposed in the effort to conceive a threshold energy for the cross-section. But no sooner was the reasonableness of the latter requirement asserted have the cross-section been found to be too large by two orders of magnitude. So finally the kinematic limits for the first reaction have to be used and the resulting cross-section said to be valid only for incident energies above  $\sim 10$  MeV.
4. Finally the exclusion requirement of the final-state neutrons was waived for the sake of a manageable calculation. The proper implementation of exclusion as sketched earlier is algebraically quite intractable; but conceptually it is simple since no ideas beyond elementary quantum mechanics are involved. Perhaps a courageous student will take up this project in the future.

## Commendation

As shown above our calculation is flawed in more ways than one. So it is not surprising that the cross-section should disagree with published results. Nevertheless discoveries were made in the stray that included the following:

1. The matrix element in (3.28) was found to depend only marginally on the coupling constants  $f_2, g_2$  and  $g_3$ . The last two were set to zero

in the calculation; and in fact if  $f_2$  were also set to zero, so that the matrix element would be

$$M \sim \langle n | \bar{\psi}_p f_1 \gamma_\lambda (1 - g_1/f_1 \gamma_5) \psi_n | p \rangle \langle e^+ | \bar{\psi}_\nu \gamma^\lambda (1 - \gamma_5) \psi_e | \bar{\nu}_e \rangle$$

instead, then the result is

$$\begin{aligned} M^2 &\sim 20.43 P_p \cdot P_e P_\nu \cdot P_n + .2704 P_p \cdot P_\nu P_e \cdot P_n \\ &+ 2.072 \times 10^6 P_e \cdot P_\nu \end{aligned}$$

which contains the same dominant  $P_p \cdot P_e P_\nu \cdot P_n$  term as before. Thus all but the 1st-class current coupling constants  $f_1$  and  $g_1$  scarcely contribute to the matrix element and hence to the cross-section. This observation is in accord with the experimental difficulty of measuring  $g_2$  and  $g_3$  (and the uncertainty in their values)<sup>3</sup>.

2. The cross-section for the reaction  $\bar{\nu}_e p \rightarrow n e^+$  is also obtained (Figure 3.8)—almost effortlessly since we already have the matrix element. Its value at very low incident energies ( $< 5$  MeV) is  $\sim 10^{-44}$  cm<sup>2</sup>, which is what should be expected.
3. It is seen that the cross-section depends sensitively on the phase space limits of the reaction. In fact it is customary in problems at higher energies to factor out  $M^2$  (cf. (3.23)) from the phase space integral and focus only on computing the latter.

Finally the model of the interaction, albeit unrealistic, allows one to tackle the problem using elementary quantum mechanics such as the bound state description and a simple field theory calculation—and to do so without very elaborate mathematics. The alternative would be to follow Mintz[26] and use a lot of complicated form factors (so that one rapidly gets lost in the formalism); or to follow Weneser[27] and use a nonrelativistic treatment (but then one would not have cause to learn quantum field theory).

---

<sup>3</sup>That 2nd-class currents do not contribute much to the cross-section is in fact peculiar to low-energy reactions.

Figure 3.8: Total cross-section for  $\bar{\nu}_e p \rightarrow n e^+$



# Appendix A

## Computer Programs

This is the REDUCE program used to calculate the trace expressions. Extensive hand calculations have been performed to verify its results.

```
ON DIV;
OPERATOR GP1,GP,VC,AC,LC,FC;
VECTOR PE,PV,PN,PP,Q;
MASS PE=ME,PV=MV,PN=M,PP=M;
MSHELL PE,PV,PP,PN;
FOR ALL P,M LET GP1(P,M)=G(L1,P)+M;
FOR ALL L,V LET VC(L,V)=G(L1,L)*F1+(G(L1,L)*G(L1,V)-
    G(L1,V)*G(L1,L))*(Q.V)*F2/(4*M);
FOR ALL L,V LET AC(L,V)=(G(L1,L)*G1+(G(L1,L)*G(L1,V)-
    G(L1,V)*G(L1,L))*(Q.V)*G2/(4*M))*G(L1,A);
INDEX V,V1;
LET (V.V)=4, (V1.V1)=4, F2=0, G2=0;
LC:=G(L1,L)*(1-G(L1,A))*GP1(PE,ME)*
    G(L1,J)*(1-G(L1,A))*GP1(PV,MV);
HC:=(VC(L,V)-AC(L,V))*GP1(PP,M)*
    (VC(J,V1)-AC(J,V1))*GP1(PN,M);
INDEX L,J;
LET Q=PV-PE;
M2:=HC*LC;
LET F1=1, G1=1.26, MV=0, ME=0.511, M=939;
M21:=M2;
;END;
```

This FORTRAN program computes the integral in (3.28). It has two quadrature routines QTRAP and QSIMP taken from W.H.Press et al, *Numerical Recipes*.

```

PROGRAM CROSS
IMPLICIT DOUBLE PRECISION (A-H,O-Z)
COMMON /BLK1/ RMN,RMP,RME,RMD
COMMON /BLK2/ PP,PV

RMN=939.6
RMP=938.3
RME=0.511
RMD=1875.6

102  A=-1.
      B=1.
11   DO 10 I=8,40
      PV=.5*I
      SUM=0.0
      DO 20 J=1,1200
      PP=0.3*J
      CALL QSIMP(A,B,S)
      SUM=SUM+S*.3
20   CONTINUE
      CS=.1227*SUM
      WRITE(19,50) PV,CS
      WRITE(6,50) PV,CS
10   CONTINUE
50   FORMAT(2E15.6)
      END

SUBROUTINE QSIMP(A,B,S)
IMPLICIT DOUBLE PRECISION (A-H,O-Z)
PARAMETER (EPS=1.E-6, JMAX=20)
OST=-1.D30
OS =-1.D30
DO 200 J=1,JMAX

```

```

        CALL TRAPZD(A,B,ST,J)
        S=(4.*ST-OST)/3.
        IF (ABS(S-OS) .LT. EPS*ABS(OS)) RETURN
        OS=S
200      OST=ST
        PAUSE 'Too many steps'
        END

SUBROUTINE TRAPZD(A,B,S,N)
IMPLICIT DOUBLE PRECISION (A-H,O-Z)
IF (N .EQ. 1) THEN
    S=0.5*(B-A)*(FUNC(A)+FUNC(B))
    IT=1
ELSE
    TNM=IT
    DEL=(B-A)/TNM
    X=A+0.5*DEL
    SUM=0.0
    DO 100 J=1,IT
        SUM=SUM+FUNC(X)
        X=X+DEL
100    CONTINUE
    S=0.5*(S+(B-A)*SUM/TNM)
    IT=2*IT
END IF
RETURN
END

FUNCTION FUNC(Z)
IMPLICIT DOUBLE PRECISION (A-H,O-Z)
COMMON /BLK2/ PP,PV
EP=SQRT(PP*PP + 880369.)
CALL ENXN(PV,PP,ENMAX,ENMIN)
FUNC=SIP(PP)*SIP(PP)*(TG(PV,PP,ENMAX,Z)
1      -TG(PV,PP,ENMIN,Z))/(EP*PV)
RETURN
END

```



```

FUNCTION TG(PV,PP,EN,Z)
  IMPLICIT DOUBLE PRECISION (A-H,O-Z)
  COMMON /BLK1/ RMN,RMP,RME,RMD
  PN=SQRT(EN*EN-RMN*RMN)
  EP=SQRT(PP*PP+RMP*RMP)
  D=(PV*EP-PV*PP*Z)/RMP
  E=(EN*EP-PN*PP*Z)/RMP
  TG1=D + RMP - E
  TG=RMP**2*(TG1**2*RME**2/(4.0*RMP) - (TG1**3)/3.0)/D
RETURN
END

```

```

SUBROUTINE ENXN(PV,PP,ENMAX,ENMIN)
  IMPLICIT DOUBLE PRECISION (A-H,O-Z)
  COMMON /BLK1/ RMN,RMP,RME,RMD
  BETA=PV/(PV+RMD)
  GAMMA=1.0/SQRT(1-BETA*BETA)
  ECM=SQRT(2.0*PV*RMD+RMD*RMD)
  EXCM=(-RME**2 - 2.0*RMN*RME + ECM*ECM)/(2.0*ECM)
  ENMIN=RMN
  THRSH=EXCM*EXCM-RMN*RMN
  IF (THRSH .LE. 0.0) THEN
    ENMAX=ENMIN
  ELSE
    ENMAX=GAMMA*(EXCM + BETA*SQRT(EXCM*EXCM-RMN*RMN))
  ENDIF
RETURN
END

```

```

SUBROUTINE ENXN1(PV,PP,ENMAX,ENMIN)
  IMPLICIT DOUBLE PRECISION (A-H,O-Z)
  COMMON /BLK1/ RMN,RMP,RME,RMD
  A1=PV*PV + 2*RMP*PV + RMN*RMN +RMP*RMP - RME*RME
  D1=(PV+RMP)**2*A1*A1
  D1=D1-4.*(RMP*RMP+2.*RMP*PV)*(A1*A1/4+PV*PV*RMN*RMN)
  IF (D1 .LE. 0.0) D1=0.

```

```

A2=2.*(RMP*RMP+2.*RMP*PV)
ENMAX=((PV+RMP)*A1+SQRT(D1))/A2
ENMIN=((PV+RMP)*A1-SQRT(D1))/A2
RETURN
END

```

```

FUNCTION SIP(Q)
  IMPLICIT DOUBLE PRECISION (A-H,O-Z)
  PI=3.1415927
  ZK1=170.0071
  ZK2=45.6572
  A=0.0108122
  B=1.76069186
  D=2.7819841
  SIP=(B*(Q*SIN(ZK1*A)*COS(Q*A)-ZK1*COS(ZK1*A)
1      *SIN(Q*A))/(ZK1*ZK1-Q*Q) + D*EXP(-ZK2*A)*(ZK2*
2      SIN(Q*A)+Q*COS(Q*A))/(ZK2*ZK2+Q*Q))
  RETURN
END

```

# Bibliography

- [1] Particle Data Group, Phys. Rev. Lett. **170B**, Apr 1986
- [2] L.Wolfenstein and E.W.Beier, Physics Today, July 89
- [3] J.Ellis, *Neutrino Masses and Neutrino Astrophysics*, IVth Telemark Conference Proceedings, 1987.
- [4] V.A.Lubimov et al, Phys. Lett. **94B**, 266 (1980) and **173B**, 485 (1986)
- [5] M.Fristchi, Phys. Lett. **173B**, 485 (1986)
- [6] K.Kawakami et al, Phys. Lett. **187B**, 198 (1987)
- [7] D.Wark et al, *Limit on Neutrino Mass from Free Molecular Tritium Beta Decay*, IVth Telemark Conference Proceedings, 1987, World Scientific Publishing Co, Singapore
- [8] M.A.Frisch et al *The IBM Neutrino Mass Experiment*, IVth Telemark Conf. Proc., 1987, p.7
- [9] B.Sur et al, *An Experiment to Determine the Mass of the Electron Antineutrino*, IVth Telemark Conf. Proc. 1987, p.1
- [10] S.S.Williams et al, *The Oxford Neutrino Mass Experiment*, IVth Telemark Conf. Proc. 1987, p.12.
- [11] R.M.Bionata et al, Phys. Rev. Lett. **58**, 1494 (1987) and T.Haines et al, IVth Telemark Conf. Proc. 1987, p.63, World Scientific, Singapore
- [12] K.Hirata et al, Phys. Rev. Lett. **58**, 1490 (1987) and E.W.Beier et al, IVth Telemark Conf. Proc. 1987, p.51, World Scientific Singapore
- [13] For a quantitative discussion see [14].
- [14] A.Burrows, IVth Telemark Conf. Proc. 1987, p.28, World Scientific, Singapore



- [15] R.J.N.Phillips, *Surveys in High Energy Physics 1988*, Vol.6, pp.1-36
- [16] G.Zacek et al, Phys. Rev D **34**, 2621 (1986)
- [17] R.Davis et al, Phys. Rev. Lett. **20**, 1205 (1968); M.L.Cherry and K.Lande Phys. Rev. D **36**, 3571 (1987)
- [18] J.N.Bahcall and R.K.Ulrich, Rev. Mod. Phys. **60**, 297 (1988)
- [19] R.Davis, Proceedings of the 13th International Conference on Neutrino Physics and Astrophysics, Neutrino '88, World Scientific, Singapore
- [20] K.S.Hirata et al, Phys. Rev. Lett. **63**, 16 (1989)
- [21] R.J.N.Phillips et al, Phys. Rev. D **34**, 980 (1980)
- [22] SLAC Z width measurement (Oh, you noticed the slip...)
- [23] T.K.Kuo and J.Pantaleone, Rev. Mod. Phys. **61**, 937, (1989)
- [24] See R.L.Liboff, *Introductory Quantum Mechanics*, Ch 13 for a discussion of the adiabatic theorem.
- [25] S.P.Mikheyev, A.Yu.Smirnov, JETP **91**, 7 (1986); L.Wolfenstein, Phys. Rev. D **17**, 2369
- [26] S.L.Mintz, Phys. Rev. C **24**, 1799 (1981) and Phys. Rev. D **13**, 639 (1976)
- [27] J.Weneser, Phys. Rev. **105**, 1335 (1957)
- [28] F.Reines et al, Phys. Rev. Lett. **45**, 1307 (1980)
- [29] Ying, W.Haxton, E.M.Henley, preprint (May 1989)
- [30] Physik Daten, ZAED 4-1, 1976, p.33
- [31] S.Gasiorowitz, *Elementary Particle Physics*, p.689 (1966)
- [32] For a background to the Dirac equation, spinors, second quantization, etc, see J.J.Sakurai, *Advanced Quantum Mechanics*, Ch 2-3, or E.G.Harris, *A Pedestrian Approach to Quantum Field Theory*, Ch 1-7. Appendix A of J.D.Byorken, S.D.Drell, *Relativistic Quantum Mechanics* will explain the notation used in the text and also provide a list of trace and spin-sum theorems.
- [33] H.Ohanian, *Modern Physics*; see pp.368 for a discussion of the deuteron bound state.

# Inverse Beta Decay (X-Sect)

